THE JOURNAL OF BIOLOGICAL CHEMISTRY
Vol. 280, No. 12, Issue of March 25, pp. 10897–10913, 2005
Printed in U.S.A.

Characterization of Oligosaccharide Ligands Expressed on SW1116 Cells Recognized by Mannan-binding Protein

A HIGHLY FUCOSYLATED POLYLACTOSAMINE TYPE *N*-GLYCAN*

Received for publication, November 19, 2004, and in revised form, January 5, 2005
Published, JBC Papers in Press, January 5, 2005, DOI 10.1074/jbc.M413092200

Motoki Terada‡§, Kay-Hooi Khoo¶‖, Risa Inoue‡§, Chun-I Chen¶‖, Kanako Yamada§, Hiromi Sakaguchi§, Naoko Kadowaki§, Bruce Yong Ma‡, Shogo Oka‡, Toshisuke Kawasaki‡, and Nobuko Kawasaki§**

From the ‡Department of Biological Chemistry, Graduate School of Pharmaceutical Sciences, Kyoto University, Kyoto 606-8501, Japan, the ¶Institute of Biological Chemistry, Academia Sinica, Taipei 11529, Taiwan, the ‖Graduate Institute of Biochemical Sciences, National Taiwan University, Taipei 106, Taiwan, and the §School of Health Sciences, Faculty of Medicine, Kyoto University, Kyoto 606-8507, Japan

Mannan-binding protein (MBP) is a C-type serum lectin and activates complement through the lectin pathway when it binds to ligand sugars such as mannose, *N*-acetylglucosamine, and fucose on microbes. In addition, the vaccinia virus carrying the human MBP gene was shown to exhibit potent growth inhibitory activity toward human colorectal carcinoma, SW1116, cells in nude mice. We have proposed calling this activity MBP-dependent cell-mediated cytotoxicity (MDCC) (Ma, Y., Uemura, K., Oka, S., Kozutsumi, Y., Kawasaki, N., and Kawasaki, T. (1999) *Proc. Natl. Acad. Sci. U. S. A.* 96, 371–375). In this study, the MBP ligands on the surface of SW1116 cells were characterized. Initial experiments involving plant lectins and anti-Lewis antibodies as inhibitors of MBP binding to SW1116 cells indicated that fucose plays a crucial role in the interaction. Subsequently, Pronase glycopeptides were prepared from whole cell lysates, and oligosaccharides were liberated by hydrazinolysis. After being tagged by pyridylamination, MBP ligand oligosaccharides were isolated with an MBP affinity column, and then their sequences were determined by mass spectrometry and tandem mass spectrometry after permethylation, in combination with endo-β-galactosidase digestion and chemical defucosylation. The MBP ligands were shown to be large, multiantennary *N*-glycans carrying a highly fucosylated polylactosamine type structure. At the nonreducing termini, Le^b/Le^a or tandem repeats of the Le^a structure prevail, a substantial proportion of which are attached via internal Le^x or *N*-acetyllactosamine units to the trimannosyl core. The structures characterized are unique and distinct from those of other previously reported tumor-specific carbohydrate antigens. It is concluded that MBP requires clusters of tandem repeats of the Le^b/Le^a epitope for recognition.

Mannan-binding protein (MBP),[1] also called mannose-binding protein (MBP) or mannan-binding lectin, is a Ca^{2+}-dependent (C-type) serum lectin and an important serum component associated with innate immunity (1–4). Human MBP is a homo-oligomer of an ~31-kDa subunit, each subunit containing a carbohydrate recognition domain followed by a short neck region on the COOH-terminal side and a collagen-like domain followed by a short cysteine-rich region on the NH_2-terminal side. Three subunits form a structural unit, and MBP normally consists of two to six structural units joined through disulfide bonds at the amino termini, the whole molecular mass being ~200–600 kDa (5, 6).

The carbohydrate specificity of MBP is rather broad (it binds to mannose, *N*-acetylglucosamine, and fucose) in accordance with the fact that MBP binds to the cell surfaces of a wide variety of pathogens (7, 8). MBP exhibits complement-dependent bactericidal activity, *i.e.* the *Escherichia coli* K12 and B strains, which have exposed *N*-acetylglucosamine and L-glycero-D-mannoheptose residues, respectively, are killed by MBP with the aid of complement (8). In addition, 1-deoxymannojirimycin (an α-mannosidase inhibitor)-treated baby hamster kidney cells, which have high mannose type oligosaccharides exposed on their surfaces, are also killed by MBP with the aid of complement (9). This complement activation pathway is called the lectin pathway (10). MBP has also been shown to function as a direct opsonin (11) and to prevent virus infection (12, 13).

* This work was supported by Grant-in-Aid for Scientific Research on Priority Areas 14082203 (to T. K.) from the Ministry of Education, Culture, Sports, Science, and Technology of Japan, by Grants-in-Aid for Scientific Research C (2)-14572054 and C (2)-16590046 (to N. K.) from the Japan Society for the Promotion of Sciences, Core Research for Evolutional Science and Technology (research area: host defense mechanism; studies on the carbohydrate-mediated host defense system) of the Japan Science and Technology Agency (to T. K.), and by the Protein 3000 project (to T. K.). Mass spectrometry analyses were performed at the Core Facilities for Proteomics Research located at the Institute of Biological Chemistry, Academia Sinica, supported by Taiwan National Science Council Grant NSC 93-3112-B-001-010-Y and the Academia Sinica, Taiwan (to K. K.). The costs of publication of this article were defrayed in part by the payment of page charges. This article must therefore be hereby marked "*advertisement*" in accordance with 18 U.S.C. Section 1734 solely to indicate this fact.

** To whom correspondence should be addressed: School of Health Sciences, Faculty of Medicine, Kyoto University, 53 Kawaharamachi, Shogoin, Sakyo-ku, Kyoto 606-8507, Japan. Tel.: 81-75-751-3934; Fax: 81-75-751-3944; E-mail: nobukokw@hs.med.kyoto-u.ac.jp.

[1] The abbreviations used are: MBP, mannan-binding protein; AAL, *A. aurantia* lectin; CID, collision-induced dissociation; ConA, concanavalin A; FACS, fluorescence-activated cell sorter; FCS, fetal calf serum; FITC, fluorescein 4-isothiocyanate; Fuc, fucose; Hex, hexose; HexNAc, *N*-acetylhexosamine; HPLC, high performance liquid chromatography; LA, lectin affinity; LacNAc, *N*-acetyllactosamine; LCA, *Lens culinaris* lectin; Le, Lewis antigen; LTA, Lotus tetragonolobus lectin; mAb, monoclonal antibody; MALDI, matrix-assisted laser desorption/ionization; MLO, MBP ligand oligosaccharides; MLO-A1, MBP ligand oligosaccharide-acidic fraction (monosialylated); MLO-N, MBP ligand oligosaccharide-neutral fraction; MS, mass spectrometry; MS/MS, tandem mass spectrometry; nano-ESI, nanoelectrospray ionization; PA, 2-aminopyridine; PBS, phosphate-buffered saline; PHA-E4, *P. vulgaris* erythroagglutinating lectin; PHA-L4, *P. vulgaris* leukoagglutinating lectin; PNA, peanut lectin; TOF, time-of-flight. All of the sugar residues have the D configuration except fucose, which has the L configuration.

In our previous studies, normal mammalian cells such as circulating blood cells did not bind MBP, probably because the surfaces of such mammalian cells are mostly covered with complex type sugar chains terminating in sialic acids and rarely with high mannose type sugar chains (14). However, malignant transformation or viral infections modify the oligosaccharide structures on cell surfaces, and aberrant glycosylation exhibited by glycolipids and glycoproteins in tumors has been implicated as an essential mechanism defining the stage, direction, and end result of tumor progression (15). Along the same lines, we found that MBP recognizes and binds specifically to the surface of human colorectal carcinoma, SW1116, cells. More interestingly, the recombinant vaccinia virus carrying the human MBP gene was demonstrated to exhibit potent growth inhibitory activity toward human colorectal carcinoma cells transplanted into KSN nude mice, when administered by intratumoral or subcutaneous injection (16). Although the mechanism of MBP-mediated tumor growth inhibition has not been clearly elucidated, we have proposed calling this activity MBP-dependent cell-mediated cytotoxicity. In addition, several other human colon adenocarcinoma cell lines have also been shown to bind MBP carbohydrate-dependently (17).

In this study, to elucidate the mechanism of MBP-dependent cell-mediated cytotoxicity, we tried to characterize the MBP ligands on the surface of SW1116 cells. The binding of the ligands to MBP is believed to be the initial signal step leading to the growth inhibition of the tumor cells. Initial hapten inhibition experiments involving various plant lectins and Lewis blood group type monoclonal antibodies (mAbs) as inhibitors of MBP-binding to SW1116 cells indicated that fucose plays an important role in the interaction. Subsequent isolation of the PA-tagged oligosaccharides ligands with an MBP-affinity column, followed by MS analysis of the ligands revealed that MBP ligands on SW1116 cells are *N*-glycans with highly fucosylated polylactosamine type structures and large molecular sizes.

EXPERIMENTAL PROCEDURES

Materials

Anti-Lewis Monoclonal Antibodies (mAbs)—Anti-human Le^a (IgG1), anti-human Le^b (IgG1), anti-human Le^y (IgG3), and anti-human sialyl-Le^a (IgG3) mAbs were obtained from SEIKAGAKU Corp. (Tokyo). The anti-human Le^x (IgM) mAb was from BD Biosciences (CA).

Isotype Control Immunoglobulins—Mouse IgG1 was obtained from MP Biomedicals Inc. (CA), mouse IgG3 from ZYMED Laboratories, Inc. (CA), and mouse IgM from BD Biosciences (CA).

Plant Lectins—Canavalia ensiformis (ConA), peanut *Arachis hypogaea* (PNA), *Lens culinaris* (LCA), *Aleuria aurantia* (AAL), and *Lotus tetragonolobus* (LTA) lectins were obtained from J-OIL Mills, Inc. (Tokyo).

Cells and Reagents for Cell Culture—SW1116 cells (ATCC CCL-233) were obtained from the American Type Culture Collection (MD). Leibovitz's L-15 medium, RPMI 1640 medium without D-glucose, and trypsin-EDTA were from Invitrogen. Fetal Calf Serum (FCS) was from JRH Biosciences (KS). Fluorescein 4-isothiocyanate (FITC) was obtained from Dojindo Laboratories (Kumamoto). FITC-labeled anti-Le^x mAb was obtained from BD Biosciences (CA), and FITC-labeled plant lectins were from J-OIL Mills, Inc. The isotope D-[1-^{3}H]glucosamine hydrochloride (TRK375) was obtained from Amersham Biosciences.

Chromatography Media and Columns—Bio-Gel P4 and Bio-Gel P10 were from Bio-Rad Laboratories, Inc. CNBr-activated Sepharose 4B was obtained from Amersham Biosciences. Dowex 50-X8 was from the Dow Chemical Company. TSKgel G2500PWXL, TSKgel G3000PWXL, TSKgel DEAE-5PW, and TSKgel Sugar AXI columns were obtained from TOSOH Corp. (Tokyo), and PALPAK type S and PALPAK type R columns were from TAKARA BIO, Inc. (Shiga). A C18 Sep-Pak cartridge (gel bed, 1 ml) was obtained from Waters Corp. (MA).

HPLC Lectin Affinity Columns—LA-AAL, LA-PHA-L4 (*Phaseolus vulgaris* leukoagglutinating lectin), and LA-PHA-E4 (*P. vulgaris* erythroagglutinating lectin) columns were obtained from J-OIL Mills, Inc.

Enzymes—Pronase was from Merck, endo-β-galactosidase (EC 3.2.1.103) from *Escherichia freundii* was from SEIKAGAKU Corp., and neuraminidase (EC 3.2.1.18) from *Arthrobacter ureafaciens* was from NACALAI TESQUE, Inc. (Kyoto).

Reference Pyridylaminated (PA) Oligosaccharides and Reference Oligosaccharides—PA-sugar chain mixture 3, PA-glucose oligomers, PA-asialoagalactotetraantennary nanosaccharide (PA-sugar chain 014), PA-trisialylated triantennary tetradecasaccharide (PA-sugar chain 024), PA-asialotetraantennary core fucosylated tetradecasaccharide (PA-sugar chain 011), PA-asialotetraantennary 3′-*N*-fucosyl-GlcNAc tetradecasaccharide (PA-sugar chain 006), and PA-lacto-*N*-fucosyl pentasaccharide (PA-sugar chain 044) were obtained from TAKARA BIO, Inc. PA-asialotriantennary undecasaccharide (PA-oligosaccharide 300.8) and PA-asialoagalactotetraantennary core fucosylated decasaccharide (PA-oligosaccharide 410.1) were from SEIKAGAKU Corp. Asialo, agalacto, bisected triantennary oligosaccharide (NGA3B) was obtained from SEIKAGAKU CORP. and was pyridylaminated as described below.

Other Chemicals—Orcin was obtained from Wako Pure Chemical Industries, Ltd. (Osaka). Hydrofluoric acid, 48 wt.% in water (48% HF), was from Sigma. D-(−)-Galactono-1,4-lactone was from NACALAI TESQUE, Inc.

Buffers

PBS (+) was 9.6 mM phosphate buffer, pH 7.5, containing 137 mM NaCl, 2.7 mM KCl, 0.7 mM $CaCl_2$, and 0.5 mM $MgCl_2$. PBS (−) was 9.6 mM phosphate buffer, pH 7.5, containing 137 mM NaCl and 2.7 mM KCl. TBS was 50 mM Tris-HCl buffer, pH 7.5, containing 150 mM NaCl. Buffer A was 20 mM Tris-HCl buffer, pH 7.5, containing 150 mM NaCl, 1% bovine serum albumin. and 0.05% Tween 20. Buffer B was 20 mM Tris-HCl buffer, pH 7.5, containing 150 mM NaCl and 2 mM EDTA. Buffer C was 20 mM Tris-HCl buffer, pH 7.5, containing 150 mM NaCl. Buffer D was 20 mM Tris-HCl buffer, pH 7.5, containing 150 mM NaCl, 1% bovine serum albumin, 10 mM $CaCl_2$, and 0.1% NaN_3. Buffer E was 20 mM Tris-HCl buffer, pH 7.5, containing 150 mM NaCl, 1% bovine serum albumin, 2 mM EDTA, and 0.1% NaN_3. Buffer F was 50 mM pyridine-acetic acid buffer, pH 5.0. Buffer G was 20 mM Tris-HCl buffer, pH 7.5, containing 150 mM NaCl and 10 mM $CaCl_2$. Buffer H was 50 mM Hepes buffer, pH 7.5, containing 150 mM NaCl and 20 mM $CaCl_2$. Buffer I was 50 mM Hepes buffer, pH 7.5, containing 150 mM NaCl and 2 mM EDTA. Buffer J was 10 mM Tris-HCl buffer, pH 7.4, containing 150 mM NaCl and 0.02% NaN_3.

Preparation of Rabbit Serum MBP and MBP-conjugated Sepharose 4B

MBP was purified from normal rabbit serum (Pel-Freez Biologicals, Inc. (AR)) using an affinity column of Sepharose 4B-mannan, as described previously (18). For the preparation of MBP-Sepharose 4B, rabbit serum MBP (3–5 mg of protein/ml of gel) was coupled to CNBr-activated Sepharose 4B according to the manufacturer's instructions.

Cell Culture

The human colorectal carcinoma cell line, SW1116 cells, was maintained by serial passages in Leibovitz's L-15 medium containing 10% heat-inactivated FCS and incubation at 37 °C with free gas exchange with atmospheric air in a standard tissue culture incubator.

Preparation of FITC-labeled MBP and FITC-labeled Anti-Lewis mAbs

FITC-labeled MBP (FITC-MBP) was prepared by conjugating the purified rabbit serum MBP with FITC (100 μg/1 mg of MBP) in 50 mM borate buffer, pH 9.2, containing 200 mM NaCl, 20 mM $CaCl_2$, and 100 mM mannose for 18 h at 4 °C. FITC-labeled anti-Lewis mAbs (except for the FITC-labeled anti-Le^x mAb) were prepared as described for the preparation of FITC-MBP in 50 mM borate buffer, pH 9.2, containing 200 mM NaCl.

Flow Cytometry Analysis: Staining of SW1116 Cells with FITC-MBP, FITC-anti-Lewis mAbs, and FITC-Plant Lectins

Reseeded SW1116 cells (5×10^6 cells/75 cm^2 flask) were grown in Leibovitz's L-15 medium supplemented with 10% heat-inactivated FCS at 37 °C for 4–5 days. After washing with PBS (−), the cells were released from the flask by incubation with trypsin-EDTA for 10 min at 37 °C. The released cells ($1–1.5 \times 10^6$ cells/ml) were dispersed as a homogeneous suspension in buffer A by thorough pipetting. Approximately 1.5×10^6 cells were washed twice with buffer B and then fixed with 2% paraformaldehyde in PBS (−) for 30 min at room temperature. After being rinsed once with buffer C and then twice with buffer D (for staining with FITC-MBP, FITC-plant lectins, and

FITC-mAbs) or buffer E (as a negative control for FITC-MBP staining), the fixed cells were incubated with 1.5 μg of each FITC-anti-Lewis mAb in a final volume of 150 μl of buffer D or 2 μg of FITC-MBP or FITC-plant lectins in 100 μl of buffer D (or buffer E, for the negative control for FITC-MBP staining) for 1 h at room temperature. After washing the cells twice with buffer D or buffer E, followed by once with buffer D, the cells were suspended in 1.0 ml of buffer D and then cell staining was analyzed with a FACScan flow cytometer with CELL Quest software (BD Biosciences).

Inhibition of FITC-MBP Binding to SW1116 Cells by Plant Lectins and Anti-Lewis mAbs

Cells (1.5×10^6 cells) fixed in 2% paraformaldehyde in PBS (−) as above were washed twice and then preincubated for 30 min at room temperature with 30 μg of protein each of various unlabeled plant lectins, or 30 and 140 μg of protein of unlabeled anti-Lewis mAbs or isotype control immunoglobulins of the respective mAbs, in 150 μl of buffer C or buffer D (as a negative control for FITC-MBP staining). To each of these suspensions, 3 μg of FITC-labeled MBP was added followed by incubation for 1 h at room temperature. After washing the cells twice with buffer D or buffer E, followed by once with buffer D, the cells (1.0×10^6) were suspended in 1.0 ml of buffer D, and then cell staining was analyzed with a flow cytometer as above.

Metabolic Labeling of SW1116 Cells with [^{3}H]Glucosamine

SW1116 cells were grown in Leibovitz's L-15 medium supplemented with 10% heat-inactivated FCS with free gas exchange with atmospheric air at 37 °C for 10 days when the cell density reached 70–80% confluence (approximately 3.5×10^7 cells/175-cm^2 culture flask). After rinsing once with PBS (−), the cells were incubated at 37 °C for 30 min under a humidified atmosphere containing 5% CO_2 in 15 ml of a mixed medium consisting of 98% RPMI 1640 medium without glucose and 2% Leibovitz's L-15 medium supplemented with 10% heat-inactivated FCS. Then, 1.85 MBq of D-[1-^{3}H]glucosamine hydrochloride dissolved in 50 μl of TBS and 1.65 mg of sodium pyruvate in 150 μl of TBS were added to the medium, and the cells were incubated at 37 °C for 20 h. ^{3}H radioactivity was determined with a liquid scintillation counter (model LSC3000; ALOKA Co., Ltd., Tokyo).

Preparation of Cell Lysates from SW1116 Cells

SW1116 cells were grown in Leibovitz's L-15 medium containing 10% heat-inactivated FCS at 37 °C for 2–3 weeks until they reached confluence through two to five passages. After rinsing the flasks once with PBS (−) containing 2 mM EDTA and twice with buffer B, the cells were removed from the flasks with cell scrapers and collected by centrifugation. The cells were washed three times with 150 mM NaCl and then homogenized in a glass-made Dounce type homogenizer (tight pestle; Wheaton Science Products) in buffer C containing 1% Triton X-100 (approximately 1×10^7 cells/ml) on ice. The homogenates were left on ice for 1 h and then centrifuged at 10,000 × *g* for 20 min. The supernatants were stored as the cell lysates at −80 °C.

Preparation of Glycopeptides from SW1116 Cell Lysates

SW1116 cell lysates were thawed and then centrifuged at 10,000 × *g* for 20 min, and the resulting supernatants were heated at 100 °C for 7 min and then lyophilized. The dried cell lysates were extracted three times with 80% ethanol followed by once with 100% ethanol and chloroform/methanol (2:1, v/v) and chloroform/methanol/H_2O (1:2:0.8, v/v/v), respectively, to remove lipids. The delipidated residues were lyophilized and digested with Pronase (sample/enzyme, 50:1 by weight) in 5.0 ml of 0.1 M borate buffer, pH 8.0, containing 10 mM $(CH_3CO)_2Ca$ for 72 h at 37 °C under a layer of toluene. During the digestion, Pronase (1/100 of the starting sample weight) was added to the incubation mixture at 24 and 48 h, respectively. The digest was centrifuged to separate a clear supernatant solution from the insoluble materials. The insoluble materials were digested again with Pronase (1/100 of the starting sample weight) for 72 h with the addition of the same amount of Pronase at 25 and 48 h, respectively. The digest was centrifuged to obtain a clear supernatant. The two clear supernatant fractions obtained after the first and second digestions were combined and lyophilized. The sample was dissolved in buffer F and then applied to a Bio-Gel P4 column (1.9 × 98 cm), which had been equilibrated with buffer F. The flow-through fraction was collected and lyophilized. The fraction was digested again with 1/100 of the starting sample weight of Pronase in 2.0 ml of 0.1 M borate buffer, pH 8.0, containing 10 mM $(CH_3CO)_2Ca$ for 72 h at 37 °C, with the addition of 1/200 of the starting sample weight of Pronase at 24 and 48 h, respectively. To the digest, trichloroacetic acid was added to a final concentration of 10%, and then the digest was left standing on ice for 30 min. The precipitate generated was centrifuged off at 10,000 × *g* for 20 min, and the resultant clear supernatant was mixed with an equal volume of aqueous saturated diethyl ether to extract the trichloroacetic acid. The extraction was repeated twice more. The aqueous phase was neutralized with ammonium bicarbonate, concentrated with a SpeedVac, and then applied to a Bio-Gel P4 column (1.9 × 98 cm). The flow-through fraction was collected as the crude glycopeptide fraction. The glycopeptide fraction was purified further on a Bio-Gel P10 column (1.9 × 100 cm) that had been equilibrated with buffer F.

Preparation of Pyridylaminated (PA) Oligosaccharides from SW1116 Glycopeptides

The glycopeptide fraction was lyophilized, dried in a vacuum desiccator over P_2O_5 for 72 h and then subjected to gas phase hydrazinolysis at 110 °C for 1 h in Hydraclub S-204 (J-OIL Mills, Inc.) to release the oligosaccharides. The released oligosaccharides were *N*-acetylated according to the manufacturer's instructions (J-OIL Mills, Inc.), the pH value of the *N*-acetylated sample solution was adjusted to 3, and then the sample was applied to a Dowex 50-X8 column. The flow-through oligosaccharide fraction from the resin was pooled and reductively aminated with 2-aminopyridine in a Palstation, model 4000 (TAKARA BIO, Inc.), using a Palstation pyridylamination reagent kit for oligosaccharide analysis (TAKARA BIO, Inc.) at 90 °C for 1 h. The PA-derivatized oligosaccharides were purified by extraction with phenol/chloroform/isoamylalchol (25:24:1, v/v/v) and with chloroform followed by gel filtration HPLC on TSKgel G2500PW$_{XL}$ (7.8 mm × 30 cm), which had been equilibrated and was eluted with 10 mM ammonium acetate buffer, pH 6.0. HPLC was performed with a Shimadzu LC-6A liquid chromatograph equipped with a fluorometer (model RF-10AXL) (Shimadzu Corp. (Kyoto)). The PA-tagged oligosaccharides were detected fluorometrically at an excitation wavelength of 320 nm and an emission wavelength of 400 nm.

Isolation of MBP Ligand Oligosaccharides on an MBP-Sepharose 4B Column

The lyophilized PA-oligosaccharides were dissolved in buffer G and then applied to an MBP-Sepharose 4B column (3 ml of gel). The column was washed with buffer G, and the bound PA-oligosaccharides were eluted with buffer H. The eluated PA-oligosaccharides were desalted by passage through a Bio-Gel P4 column (1 × 30 cm) that had been equilibrated with buffer F, and the purified MBP-binding oligosaccharides were designated as MBP ligand oligosaccharides (MLO).

Separation of Acidic and Neutral Oligosaccharides

The lyophilized PA-tagged MLO were dissolved in H_2O and then applied to a TSKgel DEAE-5PW column (7.8 mm × 7.5 cm) that had been equilibrated with eluent A (aqueous NH_3, pH 9.0). After sample injection, the column was eluted with a linear gradient of 0–50% of eluent B (0.25 M ammonium acetate, pH 8.0) over 10 min, and then with eluent A/eluent B (50:50, v/v) for 15 min, followed by 100% eluent B for 35 min at a flow rate of 1.0 ml/min at room temperature. PA-sugar chain mixture 3, a mixture of a series of oligosaccharides containing zero to four sialic acid residues/chain, was used as reference sugars.

Gel Permeation HPLC of MLO

^{3}H-Labeled PA-MLO was analyzed on a tandemly connected dual TSKgel G3000PW$_{XL}$ column (7.8 mm × 30 cm x 2) that had been equilibrated and was eluted with 10 mM ammonium acetate buffer, pH 6.0, and acetonitrile (70:30, v/v) at a flow rate of 0.5 ml/min at room temperature.

Amide Column HPLC of MLO

^{3}H-Labeled PA-MLO was applied to an amide column (4.6 mm × 25 cm; PALPAK type S) that had been equilibrated with eluent A (200 mM acetic acid-trimethylamine buffer, pH 7.3, and acetonitrile (35:65, v/v). Oligosaccharides were eluted with a linear gradient of eluent B (200 mM acetic acid-trimethylamine buffer, pH 7.3, and acetonitrile (50:50, v/v), from 0 to 100%, over 50 min and then 100% of eluent B for 100 min at a flow rate of 1.0 ml/min at 40 °C.

Lectin Affinity HPLC

The oligosaccharide fraction obtained on C18 Sep-Pak cartridge fractionation of the endo-β-galactosidase digest of ^{3}H-labeled PA-MLO was analyzed by lectin affinity HPLC on LA-PHA-E4, LA-PHA-L4, and LA-AAL columns. The eluents used for the LA-PHA-L4 and LA-PHA-E4

columns were as follows: eluent A, 50 mM Tris-H_2SO_4 buffer, pH 8.0, and eluent B, 50 mM Tris-H_2SO_4 buffer, pH 8.0, and 0.1 M potassium tetraborate. The LA-PHA-E4 HPLC column was equilibrated with eluent A, and the oligosaccharides were eluted with a linear gradient of 0–100% of eluent B in 25 min and 100% eluent B for 15 min at a flow rate of 0.5 ml/min at room temperature. The LA-PHA-L4 column was equilibrated with eluent A, and after injection of a sample, the oligosaccharides were eluted with 100% eluent A for 5 min, then a linear gradient of 0–100% of eluent B over 15 min, and finally 100% eluent B for 10 min at a flow rate of 0.5 ml/min at room temperature. The fractions were collected at 0.25 ml/tube, and an aliquot of each fraction was used for determination of ^3H radioactivity. The LA-AAL column was equilibrated with eluent A, 50 mM Tris-H_2SO_4 buffer, pH 7.3. After injection of a sample, the column was eluted with 100% of eluent A for 3 min, then 100% of eluent B (50 mM Tris-H_2SO_4 buffer, pH 7.3, and 5 mM fucose) from 3 to 13 min, and finally 100% of eluent A from 13 to 50 min at a flow rate of 0.5 ml/min at room temperature. The fractions were collected at 0.15 ml/tube, and an aliquot of each fraction was used for determination of ^3H radioactivity.

Removal of Fucose Residues by HF Treatment

To a lyophilized sample, 20 μl of 48% HF was added, and then the mixture was left at 4 °C for 48 h. At the end of the reaction, HF was removed off with N_2 gas.

Endo-β-galactosidase Digestion of ^3H-labeled PA-MLO

^3H-Labeled PA-MLO (approximately 1 μg of mannose equivalent) was digested with 25 milliunits of endo-β-galactosidase from *E. freundii* in 20 μl of 0.2 M sodium acetate buffer, pH 5.8, containing 20 mM D-(−)-galactono-1,4-lactone at 37 °C for 48 h under a layer of toluene, according to the conditions described by Fukuda *et al.* (19). After heating at 100 °C for 3 min, the digest was lyophilized.

Fractionation of the ^3H-labeled PA-MLO on a C18 Sep-Pak Cartridge after Endo-β-galactosidase Digestion

The digest was applied to a C18 Sep-Pak cartridge that had been washed sequentially with methanol, acetonitrile, and H_2O. The cartridge was eluted with 3 ml each of H_2O, 50% acetonitrile in 5% acetic acid, and 100% acetonitrile in 5% acetic acid in that order, each eluate being pooled and lyophilized.

Neuraminidase Digestion

The acidic fraction of ^3H-labeled PA-MLO (approximately 2–3 μg of mannose equivalent) was digested with 50 milliunits of neuraminidase (EC 3.2.1.18) from *A. ureafaciens* in 50 μl of 60 mM sodium acetate buffer, pH 4.5, at 37 °C for 18 h. After heating at 100 °C for 3 min, the sample was lyophilized.

Carbohydrate Analyses of Oligosaccharides

PA-tagged oligosaccharides were subjected to gas phase hydrolysis in 4 N HCl and 4 N trifluoroacetic acid (50:50, v/v) using a glass-made flask under a N_2 atmosphere at 100 °C for 4 h, according to information from TAKARA BIO, Inc. (20), and an aliquot of the hydrolysate was used for the estimation of PA-tagged reducing terminal sugars. The rest of the hydrolysate was lyophilized and reductively aminated with 2-aminopyridine in a Palstation under the same conditions as described above except that samples were heated at 90 °C for 20 min with a Palstation pyridylamination reagent kit for monosaccharide analysis. Analysis of PA-monosaccharides was carried out on a TSKgel sugar AXI column (4.6 mm × 15 cm) essentially according to the method described by Suzuki *et al.* (21). The column was equilibrated and eluted with 0.7 M borate/KOH buffer, pH 9.0, and acetonitrile (9:1, v/v) at 65 °C at a flow rate of 0.3 ml/min. PA-sugars were detected as fluorescence at an excitation wavelength of 310 nm and an emission wavelength of 380 nm. Hexose was determined by means of the orcinol reaction (22) with a slight modification for a small scale sample. Orcin (6.4 mg) was dissolved in 400 μl of ice-cold H_2O, and then the solution was mixed vigorously with 3.0 ml of ice-cold 60% H_2SO_4 (orcinol reagent). To the sample dissolved in 5 μl of H_2O, 170 μl of the orcinol reagent was added, and then the mixture was heated at 80 °C for 15 min. The mixture was rapidly cooled down to room temperature, and then the absorbance at 425 nm was determined. A standard curve was drawn using 0–1.0 μg of mannose. Sialic acid was determined by a fluorometric HPLC method involving *N*-propionylneuraminic acid as an internal standard according to the method of Ito *et al.* (23). *N*-Propionylneuraminic acid was kindly donated by Dr. Kiyoshi Ikeda (University of Shizuoka). Sialic acid was liberated from oligosaccharides by heating a sample in 0.1 N H_2SO_4 at 80 °C for 1.5 h, and determined using a C18 column (PALPAK type R, 4.6 mm × 25 cm).

Preparation of MLO for Mass Spectrometric (MS) Analysis

To prepare the PA-tagged MLO samples for MS analysis, SW1116 cells were grown in Leibovitz's L-15 medium with no radioactive sugar added. The SW1116 cell lysates prepared from 82 culture flasks (175 cm^2, each containing approximately 4.5×10^7 cells) were delipidated, and the delipidated materials were subjected to extensive digestion with Pronase as described above. The preparation of PA-tagged MLO and their subfractions, *i.e.* neutral (MLO-N) and acidic (MLO-A1) fractions, was carried out as described above for [^3H]glucosamine-labeled PA-tagged MLO. This procedure was repeated two more times. An aliquot of each of PA-MLO-N and PA-MLO-A1 was subjected to MS analysis, and another aliquot of PA-MLO (MLO-N and MLO-A1) was digested with endo-β-galactosidase as described above. The digests were fractionated into H_2O and 50% acetonitrile eluates with a C18 Sep-Pak cartridge and then used for MS analysis. All samples were permethylated using the NaOH/dimethyl sulfoxide slurry method described by Dell *et al.* (24).

MS Analysis

For MALDI-TOF MS glycan profiling, the permethyl derivatives in acetonitrile were mixed 1:1 with 2,5-dihydroxybenzoic acid matrix (10 mg/ml in acetonitrile), spotted onto the target plate, air-dried, and recrystallized on-plate with ethanol whenever necessary. Data acquisition was performed manually with a benchtop M@LDI LR system (Micromass) operated in the reflectron mode. For the 2,5-dihydroxybenzoic acid matrix, the coarse laser energy control was set at high and finely adjusted using the percent slider according to the sample amount and spectra quality. Laser shots (5 Hz, 10 shots/spectrum) were accumulated until a satisfactory signal to noise ratio was achieved when combined and smoothed. Glycan mass profiling was also performed with a dedicated Q-TOF Ultima MALDI instrument (Micromass), in which case the permethylated samples in acetonitrile were mixed 1:1 with α-cyano-4-hydrocinnamic acid matrix (in acetonitrile and 0.1% trifluoroacetic acid, 99:1, v/v) for spotting onto the target plate. The nitrogen UV laser (337 nm wavelength) was operated at a repetition rate of 10 Hz and full power (300 μJ/pulse). MS survey data were manually acquired, and the decision to switch to the CID MS/MS acquisition mode for a particular parent ion was made on the fly upon examination of the summed spectra. Argon was used as the collision gas with a collision energy manually adjusted (between 50 and 200 V) to achieve the optimum degree of fragmentation for the parent ion under investigation.

Off-line nanoelectrospray (nano-ESI) using the borosilicate metal-coated glass capillary option was performed with a Q-TOF Ultima API instrument (micromass) equipped with a nanoflow source, mainly for CID MS/MS analysis of permethylated glycan samples. The capillary voltage was set at about 1.0~1.2 kV. The cone voltage was set at 50 V for normal operation but increased to 100–150 V to induce source fragmentation. Either protonated and/or sodiated doubly charged parent ions may be selected for MS/MS, with argon as the collision gas (~4.0×10^{-5} mbar). A collision energy setting of 20~40 eV was usually sufficient for doubly protonated species, but 60~80 eV was needed for singly and double sodiated parent ions. Permethylated samples were dissolved in 50% acetonitrile and 0.2% formic acid solvent, and a 2-μl aliquot was typically loaded into the capillary for nano-ESI analysis.

RESULTS

Characterization of MBP Binding to SW1116 Cells

As we have shown previously, SW1116 cells bind to FITC-labeled MBP strongly in the presence of 10 mM $CaCl_2$. The binding is calcium-dependent because the binding is inhibited completely in the presence of EDTA, and the binding is sugar-specific because the addition of ligand sugars (mannose and *N*-acetylglucosamine, 20 mM) inhibits the binding strongly, whereas the addition of a nonligand sugar, *N*-acetylgalactosamine, at the same concentration does not inhibit the binding at all (16). These results suggest strongly that there are carbohydrates on the surface of SW1116 cells which bind specifically to MBP (MBP ligands).

To understand the properties of MBP ligands on the surface of SW1116 cells, we carried out FACS analysis. Upon incuba-

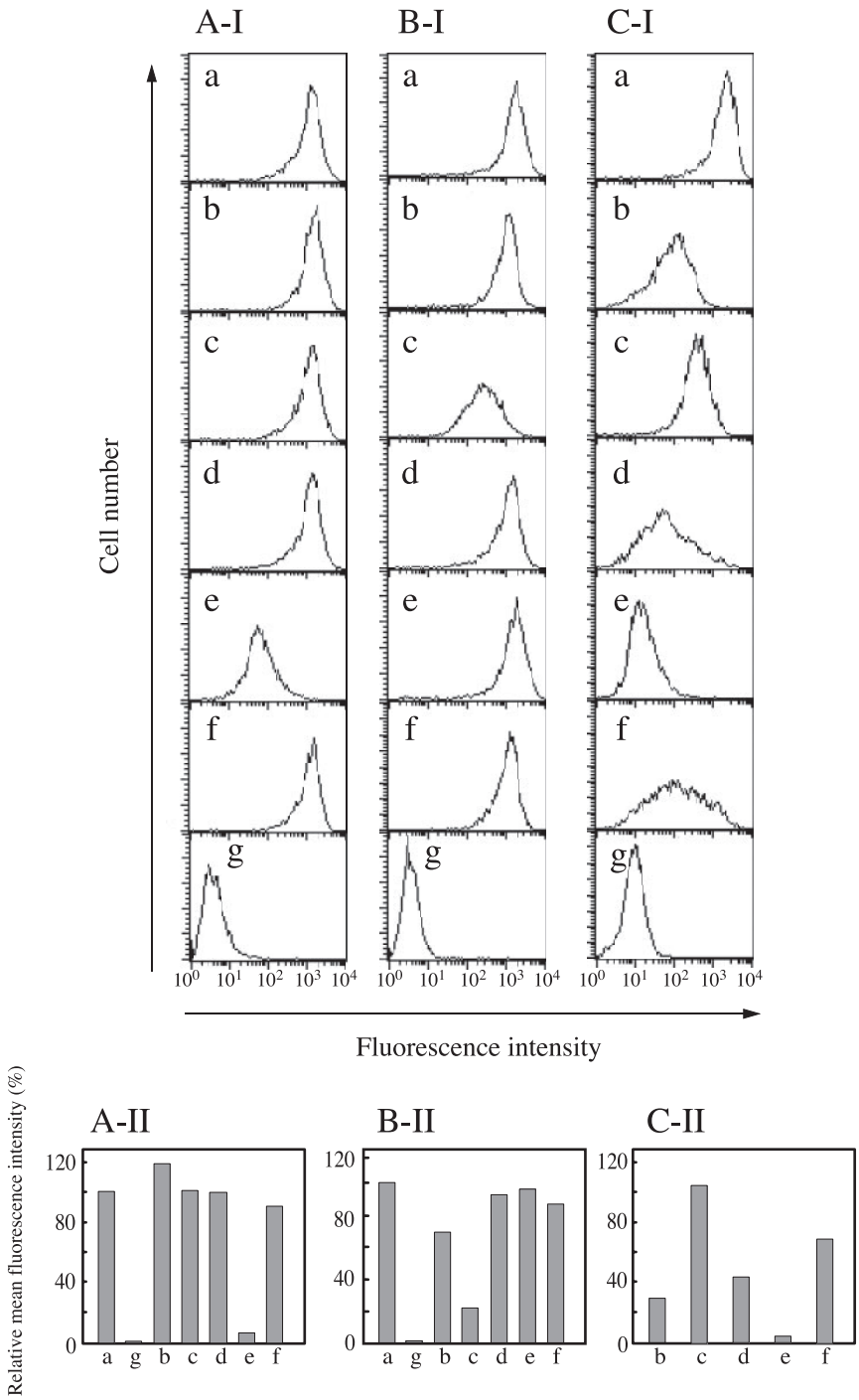

FIG. 1. **Flow cytometry analyses of FITC-labeled MBP binding to SW1116 cells.** *A-I*, effects of plant lectins on FITC-MBP binding to SW1116 cells. The cells were preincubated with 30 μg of plant lectins (*b*, ConA; *c*, LCA; *d*, PNA; *e*, AAL; *f*, LTA) or buffer alone (*a*, buffer D; *g*, buffer E) for 30 min and then stained by incubation with 3 μg of FITC-MBP in the presence of 10 mM $CaCl_2$ (buffer D) for 1 h at room temperature. Cell staining was analyzed with a flow cytometer. *A-II*, relative intensity of the cell staining with FITC-MBP after preincubation with the various plant lectins, taking the staining with FITC-MBP preincubated with buffer D alone as 100%. The *symbols* in the *panels* are as given in the legend to *A-I*. *B-I*, effects of anti-Lewis mAbs on FITC-MBP binding to SW1116 cells. The cells were preincubated with 140 μg of anti-Lewis mAbs (*b*, anti-human Le^a; *c*, anti-human Le^b; *d*, anti-human Le^x; *e*, anti-human Le^y; *f*, anti-human sialyl-Le^a) or buffer alone (*a*, buffer D; *g*, buffer E) for 30 min and then stained with 3 μg of FITC-MBP in the presence of 10 mM $CaCl_2$ (buffer D) for 1 h at room temperature. Cell staining was analyzed with a flow cytometer. *B-II*, relative intensity of the cell staining with FITC-MBP after preincubation with the various anti-Lewis mAbs, taking the staining with FITC-MBP preincubated with the respective isotype control immunoglobulins as 100%. The *symbols* in the *panels* are as given in the legend to *B-I*. *C-I*, expression of Lewis antigens on SW1116 cells. Cells were incubated with 1.5 μg of FITC-antiLewis mAbs (*b*, anti-human Le^a; *c*, anti-human Le^b; *d*, anti-human Le^x; *e*, anti-human Le^y; *f*, anti-human sialyl-Le^a) or 3 μg of FITC-MBP in the presence (*a*, buffer D) or absence (*g*, buffer E) of 10 mM $CaCl_2$ for 30 min at room temperature. Cell staining was analyzed with a flow cytometer. *C-II*, relative intensity of the cell staining with various FITC-anti-Lewis mAbs, taking the staining with anti-Le^b mAb as 100%. The *symbols* in the *panels* are as given in the legend to *C-I*.

tion of SW1116 cells with FITC-labeled rabbit serum MBP (FITC-MBP) for 1 h at room temperature, the fluorescence intensity of the cells increased more than several hundred times over the EDTA control, indicating the strong binding of MBP to SW1116 cells (Fig. 1*A*). Then, we tested various plant lectins as inhibitors of MBP binding, taking advantage of the carbohydrate binding specificity of plant lectins (25–27). ConA binds specifically to biantennary type, high mannose type, and hybrid type *N*-glycans, which have more than two α-Man with free C-3, C-4, and C-6 OH residues. LCA recognizes α-Man and α-Glc residues. PNA binds to Gal residues, exhibiting particularly high affinity to the Galβ1–3GalNAc structure. AAL recognizes the α-Fuc residues in type 1 and 2 structures (see Table I) and binds strongly to the Fucα1–6 structure, followed by the Fucα1–2 and Fucα1–3 structures. LTA binds to type 2 chains, strongly to the Le^y epitope, and weakly to the Le^x epitope, and essentially does not bind to the type 1 structure, Le^a and Le^b epitopes. SW1116 cells were preincubated with these plant lectins for 30 min at room temperature, prior to the addition of FITC-MBP. After incubation at room temperature for 1 h, SW1116 cells were subjected to FACS analysis as described under "Experimental Procedures." As might be expected, PNA, a Gal-specific lectin, did not inhibit the binding at all. However, to our surprise, lectins that recognize and bind Man residues such as ConA and LCA did not inhibit the binding significantly. In contrast, a Fuc-binding lectin, AAL, inhibited the binding markedly. These results indicated that manno-oligosaccharide structures, which are frequently the natural ligands on pathogenic microorganisms, are not associated with the tumor recognition by MBP, and instead Fuc-containing sugar chains

TABLE I
Structures of the Lewis blood group type epitopes

Type 1 (Galβ1–3GlcNAc)	Type 2 (Galβ1–4GlcNAc)
Le^a Galβ1–3GlcNAcβ1- 4 | Fucα1	Le^x Galβ1–4GlcNAcβ1- 3 | Fucα1
Le^b Galβ1–3GlcNAcβ1- 2 | Fucα1, 4 | Fucα1	Le^y Galβ1–4GlcNAcβ1- 2 | Fucα1, 3 | Fucα1
Sialyl-Le^a (CA19–9) Galβ1–3GlcNAcβ1- 3 | NeuAcα2, 4 | Fucα1	

such as blood group type substances may play important roles in the recognition of SW1116 cells. Another interesting point is the negligible inhibition by LTA compared with that by AAL, both being Fuc-binding lectins. This difference may be explained by the linkage specificities of these lectins described above, suggesting that the MBP ligands on SW1116 cells have the type 1 structure rather than the type 2 structure. The results of these inhibition studies were completely consistent with those of binding studies involving FITC-labeled lectins. Upon incubation of SW1116 cells with 2 μg of various FITC-lectins as described under "Experimental Procedures," the relative binding activity of AAL was found to be about 3.5 times higher than that of MBP, whereas those of the other lectins, *i.e.* ConA, LCA, and LTA, were less than one-fifth that of MBP, and PNA did not bind to SW1116 cells at all (data not shown).

In the next experiment, we characterized the nature of the fucose residues to which MBP is assumed to bind selectively by using various anti-Lewis mAbs as inhibitors. As shown in Fig. 1*B*, the anti-Le^b mAb inhibited the MBP binding most effectively and dose-dependently, followed by the anti-Le^a mAb, whereas the anti-Le^x and anti-Le^y mAbs did not inhibit the binding significantly even when a large amount of antibodies (140 μg) was added. These results are consistent with the potent inhibitory activity of AAL, suggesting that MBP recognizes and binds fucose residues that are the constituents of Le^b and Le^a blood group epitopes. The fact that Le^b and Le^a blood group epitopes belong to type 1 chains and not to type 2 chains suggested two possibilities: MBP binds to type 1 chains but not to type 2 chains, or only type 1 chains are present on the surface of SW1116 cells. This was examined by measuring the direct binding of FITC-labeled anti-Lewis mAbs (1.5 μg) to SW1116 cells, as described under "Experimental Procedures." As shown in Fig. 1*C*, the anti-Le^b mAb bound to the cells most strongly (the binding being almost the same as MBP binding) giving a single peak with good symmetry. The anti-sialyl-Le^a mAb showed the second highest average binding to SW1116 cells, although the cells were markedly heterogeneous with respect to the binding levels. The anti-Le^a and anti-Le^x antibodies showed almost half the levels of staining with the anti-Le^b mAb, but the histograms were rather broad. The anti-Le^y mAb showed almost negligible staining. It should be noted here that equivalent amounts of all isotype controls for these monoclonal antibodies, *i.e.* mouse IgG1, IgG3, and IgM, did not show any specific interactions with SW1116 cells under the conditions used.

These results together with the inhibition experiments described above suggested that SW1116 cells express type 1 sugar chains as predominant carbohydrate components, which include

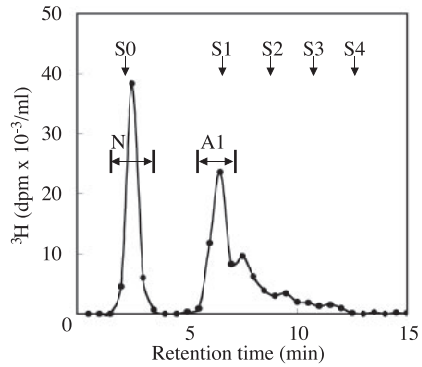

FIG. 2. **Anion exchange HPLC of [^{3}H]glucosamine-labeled MLO.** ^{3}H-Labeled MLO was applied to a TSKgel DEAE-5PW column (7.8 mm × 7.5 cm) that had been equilibrated with eluent A (aqueous NH_3, pH 9.0). The oligosaccharides were eluted with a linear gradient of eluent B (0.25 M ammonium acetate, pH 8.0), from 0 to 50%, over 10 min, and 50% from 10 to 25 min at a flow rate of 1.0 ml/min at room temperature. Fractions were collected at 0.5 ml/tube, and an aliquot of each fraction was used for determination of ^{3}H radioactivity. The neutral fraction (*N*; retention time, 1.5–3 min) and acidic fraction (*A1*; retention time, 5–7 min), as indicated by *bars*, were separately pooled and named MLO-N and MLO-A1, respectively. The *arrows* indicate the elution positions of reference PA-oligosaccharides, *S0*, nonsialylated biantennary oligosaccharide; *S1*, monosialylated biantennary oligosaccharide; *S2*, disialylated biantennary oligosaccharide; *S3*, trisialylated triantennary oligosaccharide; *S4*, tetrasialylated triantennary oligosaccharide.

TABLE II
Carbohydrate compositions and reducing end sugars of MLO-N

1 μg (mannose equivalent) of PA-tagged MLO-N was subjected to gas phase acid hydrolysis in 4 N HCl and 4 N trifluoroacetic acid (50:50, v/v). An aliquot of the hydrolysate was used for the determination of reducing terminal PA-sugars on a TSKgel sugar AXI column. The rest of the hydrolysate was pyridylaminated, and PA-monosaccharides were analyzed on the same column. These data have been corrected for destruction of sugars during hydrolysis, taking into account the results of an experiment involving PA-sugar chain 001 (TAKARA BIO, Inc.) as a control.

	Reducing end sugars relative ratio	Total sugars relative ratio	mol of sugar per mol of reducing end GlcNAc
	%	%	
GalNAc	0	0	0
GlcNAc	90.4	39.7	26.1
Gal	0	33.5	22.1
Fuc	0	22.0	14.5
Man	0	4.8	3.1
Unidentified	9.6	0	0
	100	100	65.8

the sialyl-Le^a, Le^a, and Le^b epitopes, and also type 2 sugar chains as minor components, which include the Le^x epitope. MBP binds selectively to fucose residues in type 1 carbohydrate chains, and the presence of sialic acid at a proximal position strongly attenuates the binding activity of the Le^a epitope. The preferential binding of MBP to type 1 chains rather than type 2 chains described here is consistent with the results of previous specificity studies involving neoglycolipids (28).

Isolation of MBP Ligands from SW1116 Cells

To understand more clearly the properties of MBP ligands on the surface of SW1116 cells, we isolated the MBP ligands, initially by means of metabolic radiolabeling, and subsequently on a larger scale without radiolabeling for chemical and mass spectrometry analyses. Typically, SW1116 cells metabolically labeled with D-[1-^{3}H]glucosamine for 20 h were collected from 34 culture flasks (175 cm^2), and the lysates were delipidated with organic solvents and then digested extensively with Pronase. The digests were applied to a Bio-Gel P4 column, and the

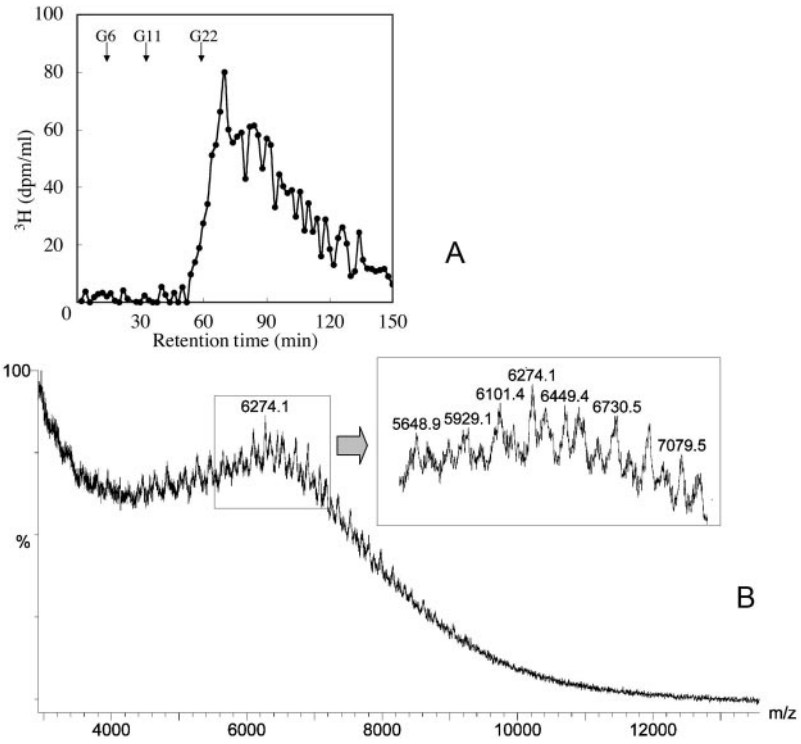

FIG. 3. **Molecular size distribution of intact MLO-N, as estimated by amide column HPLC and MALDI-TOF MS analysis.** *A*, [^{3}H]glucosamine-labeled MLO-N was applied to an amide HPLC column (4.6 mm × 25 cm, PALPAK type S) that had been equilibrated with eluent A (200 mM acetic acid-triethylamine buffer, pH 7.3 and acetonitrile, 35:65, v/v). The oligosaccharides were eluted with a linear gradient of eluent B (200 mM acetic acid-triethylamine buffer, pH 7.3 and acetonitrile, 50:50, v/v), from 0 to 100%, over 50 min and then 100% of eluent B, from 50 to 150 min, at a flow rate of 1.0 ml/min at 40 °C. Fractions were collected at 1.0 ml/tube, and an aliquot of each fraction was used for determination of ^{3}H radioactivity. *Arrows* indicate the elution positions of reference PA-glucose oligomers, *G6*, 6mer of glucose unit; *G11*, 11mer of glucose unit; *G22*, 22mer of glucose unit. *B*, nonradiolabeled, permethylated intact MLO analyzed by MALDI-TOF MS in the linear mode, showing the complexity of signals at *m/z* 4200–9000 with distinctive mass intervals corresponding to Fuc, and Hex-HexNAc differences, as shown in an expanded view (*inset*), for the signal clusters peaking at around *m/z* 6200. The signals were not of sufficient quality, resolution, and accuracy in the linear TOF mode to allow molecular composition assignment.

glycopeptide fraction eluted at the void volume was then fractionated on a Bio-Gel P10 column. Essentially all radioactivity was recovered as a single peak at a slightly retarded position, with significant tailing. The corresponding glycopeptide fractions were pooled and subjected to hydrazinolysis followed by pyridylamination as described under "Experimental Procedures." After purification by gel filtration on a TSKgel G2500PW$_{XL}$ column, the purified PA-oligosaccharides were subjected to affinity chromatography on an MBP-Sepharose 4B column in the presence of 20 mM $CaCl_2$ (buffer H). A predominant portion of the radioactivity was recovered in the pass-through fraction, but a definite amount of radioactivity (approximately 5.9%) was bound to the column and eluted with the elution buffer (buffer I). This fraction is designated as MBP ligand oligosaccharides (MLO).

Upon ion exchange chromatography on a DEAD-5PW column, MLO was fractionated into a neutral pass-through fraction (MLO-N, 38% by radioactivity) and two or three acidic fractions, the elution position of the major acidic component (MLO-A1, 36% by radioactivity) corresponding to that of the monosialylated oligosaccharide, as shown in Fig. 2. The sugar compositions and reducing terminal sugars of these fractions were then analyzed (Table II). More than 90% of the reducing terminal sugar was identified as GlcNAc, indicating that MLO-N consists mostly of *N*-glycans. The major constituents are GlcNAc, Gal, and Fuc in a molar ratio of 39.7%, 33.5%, and 22.0%, respectively, whereas Man is present as a minor component (4.8%). Thus, there are 26, 22, 15, and 3 mol of GlcNAc, Gal, Fuc, and Man, respectively, per mol of reducing end GlcNAc, suggesting that MLO have unusually long carbohydrate chains. For a nonradiolabeled sample, ~1.72 mg of mannose equivalent of glycopeptides was isolated from SW1116 cells collected from 82 culture flasks (175 cm^2). Upon fractionation on an affinity column of MBP-Sepharose, 41 μg of mannose equivalent of PA-MLO was isolated, of which 18 μg of mannose equivalent was recovered as MLO-N and 13 μg as MLO-A1.

Characteristics of Intact MBP Ligands

Molecular Size Distribution—HPLC analysis on an amide column (Takara PALPAK type S) revealed that MLO-N comprised a series of oligosaccharides with slightly different molecular sizes in the high molecular weight range of over 20 glucose units (Fig. 3*A*). More indicative estimation of size was possible by MALDI-MS analysis of the intact MLO-N sample after permethylation. In the high mass range with the linear mode, a cluster of signals was observed between *m/z* 4200 and 9000 (Fig. 3*B*). Throughout this region, peaks differing by a Fuc or Fuc-(Hex-HexNAc) unit difference were observed (Fig. 3*B*, *inset*). Because of the extreme heterogeneity and compositional permutation, further compounded by the possibility of in source prompt fragmentation, the exact molecular composition of each of the detected peaks could not be deduced accurately. However, assuming a basic PA-tagged trimannosyl core structure, the *m/z* values at around 4200 correspond to about 5 Gal-GlcNAc with 4 Fuc, whereas those extending to about *m/z* 9000 can correspond to a maximum number of 13 Gal-GlcNAc with 11 Fuc. These values translate into a molecular mass distribution of about 3400–7400 Da for the native, nonmethylated MLO-N, peaking at about a molecular size corresponding to ~25–35 glycosyl residues.

Nonreducing Terminal Sequence—In the lower mass range, prompt fragment ions were afforded on direct MALDI-MS analysis of permethylated MLO-N, which, with a MALDI-Q/TOF instrument, could be further selected for CID MS/MS. Alternatively, by raising the cone voltage, source fragmentation could also be induced with an off-line nanospray source, which could likewise be selected for CID MS/MS with an ESI-Q/TOF. The latter tends to give clearer signals for the low mass end compared with the spectrum afforded on MALDI-MS, which gave instead more distinctive fragment ion signals at higher *m/z*, *i.e.* up to about *m/z* 3000. Combining the two sets of data, a series of fucosylated, nonreducing terminal oxonium type fragment ions (29) including up to 5 Hex-HexNAc units was detected (Fig. 4). The signal at *m/z* 464 corresponds to terminal Hex-

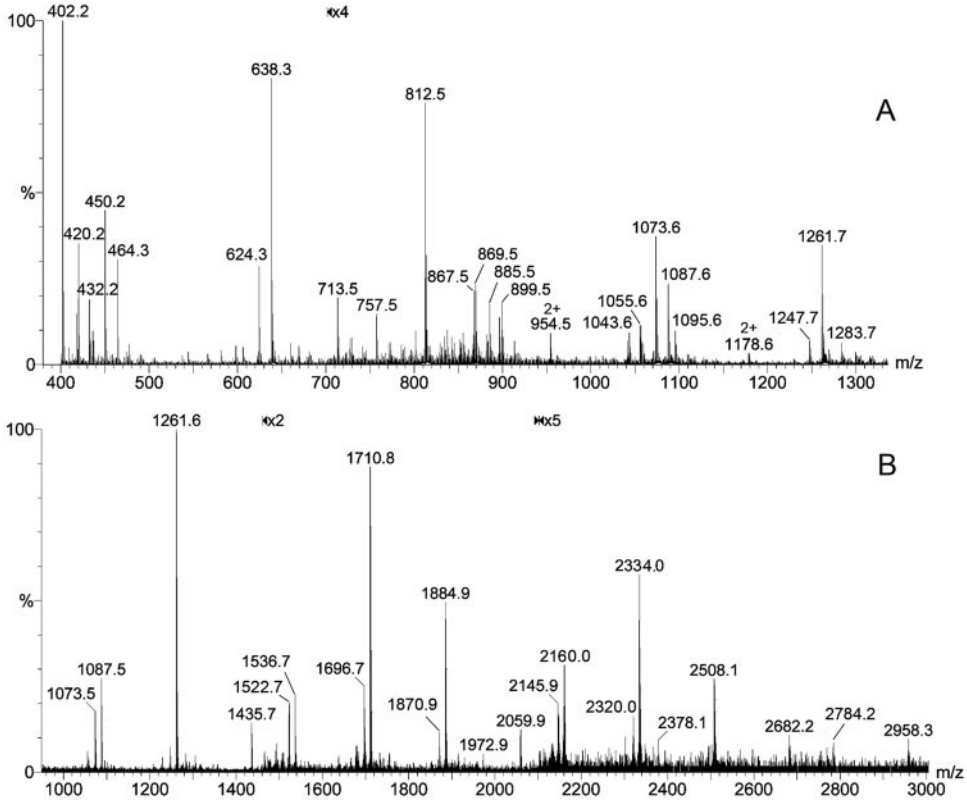

FIG. 4. **Nonreducing terminal fragment ions afforded on MS analyses of intact, permethylated MLO-N.** *A*, cone voltage fragmentation by off-line nano-ESI-MS gave singly charged oxonium type ions for $Fuc_{0-2}Hex_1HexNAc_1^+$ at *m/z* 464, 638, and 812, and $Fuc_{1,2}Hex_2HexNAc_2^+$ at *m/z* 1087, and 1261, respectively. Larger fragments occurred as doubly charged, sodiated oxonium ions, *e.g.* at *m/z* 954 and 1178 for $Fuc_3(Hex\text{-}HexNAc)_{3,4}^+$, respectively. *B*, in source prompt fragmentation afforded on MALDI-MS analysis, which gave singly charged oxonium type fragment ions similar to in *A* but up to a mass range of *m/z* 3000. The signals at *m/z* 1536, 1710, 1884, and 2059 correspond to $Fuc_{1-4}(Hex\text{-}HexNAc)_3^+$, those at *m/z* 2160, 2334, 2508, and 2682 to $Fuc_{2-5}(Hex\text{-}HexNAc)_4^+$, and those at *m/z* 2784 and 2958 to $Fuc_{3,4}(Hex\text{-}HexNAc)_5$, respectively. Signals at 14 units lower than these assigned could be attributed to secondary loss of glycosyl residue(s) from a larger fragment. The fragment ions are further alluded to under "Results" and in Fig. 5.

$HexNAc^+$ and was relatively much less abundant compared with mono- and difucosylated terminal $Hex\text{-}HexNAc^+$ (*m/z* 638, 812). Larger fragment ions could be assigned to additional internal Hex-(±Fuc)HexNAc repeating units, as confirmed by further MS/MS analyses.

Exemplary MS/MS spectra for $(Hex\text{-}HexNAc)_3^+$ with 2, 3, and 4 Fuc are shown in Fig. 5. In general, the more abundant species carried the same number of Fuc as the number of Hex-HexNAc units. Maximal fucosylation occurred when all internal Hex-HexNAc units were monofucosylated and were terminated at the nonreducing end with a difucosylated unit. "Under"-fucosylated fragments can have one or more Fuc missing in any one of the internal Hex-HexNAc units, but the nonreducing terminal units were shown by MS/MS to be mostly mono- or difucosylated, giving ions at *m/z* 638 and 812, respectively. Accompanying signals that correspond to further elimination of a Fuc 3-linked to the HexNAc oxonium (*m/z* 432 and 606, from *m/z* 638 and 812, respectively) were barely detected, indicating the presence of a small amount of nonreducing terminal $Le^{x/y}$ unit. In contrast, an intense fragment ion was observed at *m/z* 402 on direct MS (Fig. 4*A*) and all MS/MS analyses, attributable to elimination of a 3-linked substituent from a fucosylated HexNAc oxonium, which could be derived from any of the Le^a units along the chain, including the terminal $Le^{a/b}$. These pseudo MS^3 analyses of the terminal sequence of MLO-N therefore firmly established its highly fucosylated nature, with predominantly the $Le^{a/b}$ epitope at the termini, consistent with the results of the initial inhibition studies on MBP binding to SW1116 cells by plant lectins and anti-Lewis mAbs.

The importance of a fucose residue for MBP binding was confirmed further by chemical defucosylation of MLO-N. After selective cleavage of fucosyl linkages with HF, a predominant portion of MLO-N no longer bound to an AAL column, concomitant with loss of binding to an MBP column (data not shown). Upon gel filtration on a TSKgel $G3000PW_{XL}$ column, the defucosylated MLO-N was eluted as a single peak at a position only slightly retarded compared with that of the untreated MLO-N (data not shown), suggesting that the main backbone chain was not significantly affected, and only branched fucoses were released on this treatment.

Chemical and Functional Analysis of Endo-β-galactosidase-digested MLO-N

The chemical data and physicochemical properties of MLO-N described above suggested that MLO-N may have high molecular mass complex type *N*-glycans, with terminal $Le^{a/b}$ epitopes on variably fucosylated type 2 polylactosamine structures $(Gal\beta1\text{–}4GlcNAc)_n$, or extended type 1 chains $(Gal\beta1\text{–}3GlcNAc)_n$, or a hybrid of the two. To delineate its fine structure further, MLO-N was digested with *E. freundii* endo-β-galactosidase, which only cleaves type 2 chains without a Fuc on the GlcNAc immediately adjacent to the cleavage site Gal, and the digest was analyzed by gel filtration on a TSKgel $G3000PW_{XL}$ column. The digestion was carried out according to the conditions of Fukuda *et al.* (19), using a higher concentration of the enzyme, with which not only linear chains but also branched chains of poly-LacNAc can be degraded. As shown in Fig. 6*A*, after digestion, the elution profile of [^{3}H]glucosamine-labeled MLO-N exhibited a heterogeneous distribu-

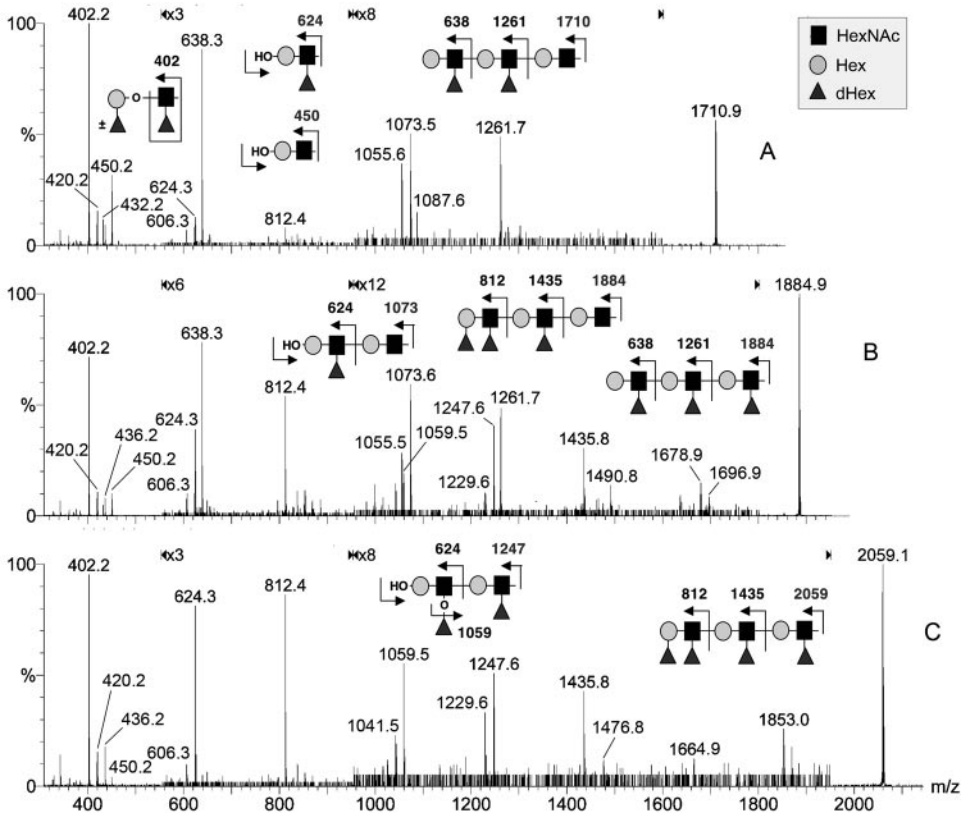

FIG. 5. **MALDI-CID MS/MS analyses of prompt fragment ions afforded on permethylated intact MLO-N.** Three representative MS/MS spectra are shown for $(Hex\text{-}HexNAc)_3^+$ containing 2, 3, and 4 Fuc, respectively (*A–C*). Assignments of major MS/MS ions are illustrated schematically, and the *symbols* used are shown as an *inset*. Further elimination of a 3-linked Fuc (minus 206 units) is indicative of terminal $Le^{x/y}$ or internal Le^x, *e.g.* *m/z* 432 (from *m/z* 638), 606 (from *m/z* 812), 1041/1055 (from *m/z* 1247/1261), 1229 (from *m/z* 1435), 1490 (from *m/z* 1696), 1678 (from *m/z* 1884), and 1853 (from *m/z* 2059), whereas similar elimination of the 3-linked substituent from $Le^{a/b}$ or any internal Le^a would yield *m/z* 402. The corresponding loss of terminal Fuc-Gal- from terminal Le^y would give the ion at *m/z* 420. Signals at 14 units lower than those assigned reflected an additional free OH group and hence were derived through further secondary cleavage, as shown schematically for *m/z* 624, 450, and 1247.

tion as to molecular size distinct from the single peak before digestion, suggesting that there are some Galβ1–4GlcNAc linkages in MLO-N. Redigestion of fraction *a* (*dotted* area) with the endo-β-galactosidase did not cause any significant further changes in the elution profile (data not shown), suggesting that a minor fraction with a molecular size corresponding to that of the undigested MLO-N remained resistant to the enzyme.

Loss of MBP Binding Functions—Interestingly, the major portion of the digest, *i.e.* fraction *b*, almost completely lost the ability to bind to an MBP column (Fig. 6*B*). This could not be explained by an accidental loss of fucose residues during the endo-β-galactosidase digestion because, as shown in Fig. 6*C*, essentially all of the radioactivity was bound to an LA-AAL column and eluted with a buffer containing fucose. It should be pointed out here that the binding affinity of carbohydrate ligands to MBP is known to depend markedly on the clustering or the topological pattern of the ligand sugars (3, 4). Therefore, it was speculated that the loss of the binding to the MBP column after endo-β-galactosidase treatment might be caused by degradation of MLO-N into oligosaccharide fragments, the size of which is below a critical value necessary for the high affinity recognition by MBP. To examine this hypothesis, we examined the molecular sizes of the digest, fraction *b*, in Fig. 6*A* on an HPLC-amide column. As shown in Fig. 6*D*, fraction *b* exhibited a distribution of molecular sizes that were much smaller than those of the original MLO-N (see Fig. 3*A*). A similar situation was observed for fraction *a* in Fig. 6*A*. Upon fractionation on an MBP column, only approximately 38% of the $[^3H]$glucosamine retained its original ability to bind to the column, whereas a major part of the fraction *a* lost the binding ability and was eluted in the pass-through fraction, although the pass-through fraction from the MBP column still bound to an AAL column (data not shown).

Identification of Released Terminal Structures—To identify the released fragments that contributed to MBP binding as well as to characterize further the endo-β-galactosidase-resistant product, the digest was fractionated on a reverse phase C18 Sep-Pak cartridge and then permethylated for MS analysis (Fig. 7). Because MLO-N was originally tagged at the reducing end with PA, the released oligosaccharides were expected to be in the washed-through fraction, whereas the PA-tagged core portion should be eluted in the 50% acetonitrile fraction. As shown in Fig. 7*A*, the aqueous wash fraction afforded a series of molecular ion signals that could be assigned as $[M+Na]^+$ of $\pm$Fuc-Hex-[(Fuc)HexNAc-Hex]$_n$, where the reducing terminal Hex corresponds to the β-Gal at which endo-β-galactosidase cleaved. Such nonreducing terminal structures containing up to 4 Lewis units could be detected. To facilitate sequence assignment, the sample was reduced further to convert the oligosaccharides into oligoglycosyl alditols and permethylated before selecting the sodiated precursors for MALDI MS/MS analyses. In addition, protonated precursors were also detected and selected for MS/MS in the nano-ESI mode to provide complementary data.

These MS/MS analyses clearly revealed a predominance of Le^a-galactitol and Le^b-galactitol structures for the smallest fragments released by endo-β-galacosidase, based on the major sodiated fragment ions detected (data not shown). Further

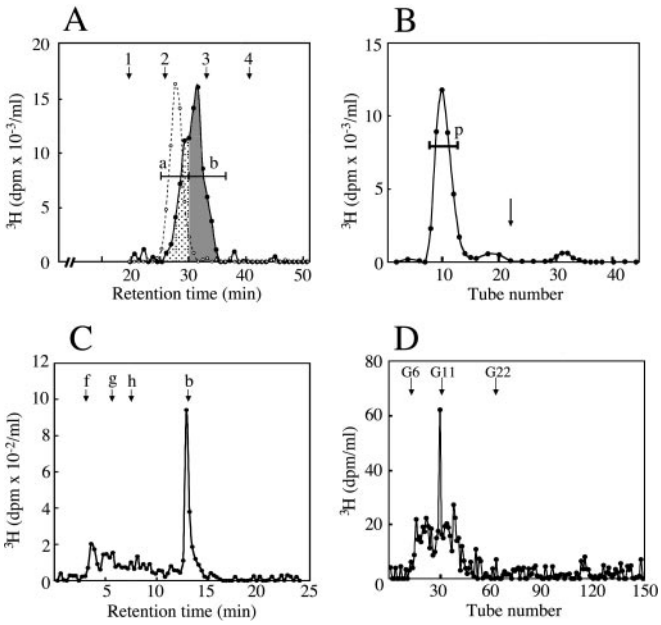

FIG. 6. **Gel permeation HPLC and lectin affinity chromatography of [^{3}H]glucosamine-labeled MLO-N after endo-β-galactosidase digestion.** *A*, ^{3}H-labeled MLO-N after endo-β-galactosidase digestion was applied to a tandemly connected dual TSKgel G3000PW$_{XL}$ column (7.8 mm × 30 cm × 2), equilibrated, and eluted with 10 mM ammonium acetate buffer, pH 6.0 and acetonitrile, 70:30, v/v at a flow rate of 0.5 ml/min at room temperature. The oligosaccharide fractions (retention time 29.6 ~ 36 min, fraction *b*), which shifted to lower molecular positions on digestion, were pooled, as indicated by the *shaded* area. The *dotted line trace* shows the elution pattern of the ^{3}H-labeled MLO-N before endo-β-galactosidase digestion, which was size-calibrated against the elution positions of reference substances, as denoted by *arrows*: *1*, polyethylene oxide (molecular weight, 250,000); *2*, polyethylene glycol (7,500); *3*, polyethylene glycol (1,000); *4*, ethylene glycol (62). *B*, the lower molecular size fractions (fraction *b* in *A*) were applied to an MBP-Sepharose 4B (0.5-ml gel) column, which had been equilibrated with buffer H. The bound oligosaccharides were eluted with buffer I at a flow rate of 4.8 ml/h at room temperature. The *arrow* denotes the start point of elution with buffer I. The MBP-nonbinding fraction (fraction *p*) was pooled as indicated by a *bar*. *C*, lectin affinity HPLC of MBP-nonbinding fractions (fraction *p* in *B*) on an LA-AAL column (4.6 mm × 15 cm). The column was equilibrated with eluent A (50 mM Tris-H_2SO_4 buffer, pH 7.3) and developed with 100% of eluent A for 3 min, then 100% of eluent B (5 mM fucose and 50 mM Tris-H_2SO_4 buffer, pH 7.3) from 3 to 13 min, and 0% eluent B and 100% eluent A from 13 to 50 min at a flow rate of 0.5 ml/min. Fractions were collected at 0.15 ml/tube. The *arrows* indicate the elution positions of reference PA-oligosaccharides, 10 pmol of each of which was injected into the columns. *b*, agalactotetraantennary core fucosylated decasaccharide; *f*, asialo, agalactotetraantennary nanosaccharide; *g*, asialotetraantennary 3′-*N*-fucosyl-GlcNAc tetradecasaccharide; *h*, lacto-*N*-fucosyl pentasaccharide. For the structures of reference PA-oligosaccharides, see the legend to Fig. 10. *D*, amide column (type S) HPLC of the MBP-nonbinding fraction (fraction *p* in *B*), performed as described in the legend to Fig. 3.

evidence was provided by nano-ESI-MS/MS analysis of the protonated parents, in which the relative abundance of terminal Le^a/Le^x was indicated by the relative abundance of ions at *m/z* 402/432 (Fig. 8*A*) and that of Le^b/Le^y by ions at *m/z* 402/606 (Fig. 8*B*).

For larger fragments, the presence of internal type 1 or Le^a units was indicated by the corresponding c and z ion pairs observed on MALDI-MS/MS analyses of the sodiated parents (Fig. 8, *C–F*). Detection of z ion, in particular, is diagnostic of a 3-linkage which favors the elimination of the glycosyl substituent, be it an entire chain or a single Fuc substituent from the HexNAc, but the MS/MS data cannot exclude the coexistence of type 2 chains or Le^x. Taken together with the data obtained on MS and MS/MS analysis of intact MLO-N described in previous sections (Figs. 4 and 5), it can be firmly concluded that the nonreducing terminal epitopes of MLO-N were predominantly Le^b and Le^a. A significant portion of these terminal epitopes appeared to be carried on extended chains carrying internal Le^a units. Although the exact distribution pattern of internal type 1 and 2 units remains to be established, it is clear that the majority of the terminal Le$^{b/a}$ epitopes that contributed to MBP binding were attached via nonfucosylated internal type 2 LacNAc units to the core structure and were thus susceptible to release on endo-β-galactosidase digestion.

Characterization of the Core Structure—MALDI-MS analysis of the C18 Sep-Pak retained fraction, in which the endo-β-galactosidase-resistant, PA-tagged core structures were expected to be recovered, afforded several major peaks that could be readily assigned (Fig. 7*B*). The $[M+Na]^+$ molecular ion signals at *m/z* 1519, 1694, 2144, 2319, and 2767 were the same as those detected for the released fragments in the washed-through fraction, some of which were carried over to the next eluted fraction. The signals at *m/z* 1261, 1435, 1885, and 2682 correspond to oxonium type in source prompt fragment ions, similar to those afforded on direct MALDI-MS analysis of intact MLO-N (Fig. 4). These fragment ions indicated that a significant amount of the resistant core structures still carried poly-Le$^{a/x}$ antennae and that the apparent lack of under-fucosylated internal LacNAc is consistent with it being otherwise susceptible to release by endo-β-galactosidase.

The rather heterogeneous nature of the resistant core structures was reflected by the multitude of molecular ion signals afforded in the mass range of *m/z* 2200–5000. Among the more prominent ones, the major signal at *m/z* 2419 could be assigned to $[M+Na]^+$ of a fucosylated trimannosyl core with an additional 4 nonreducing terminal GlcNAc attached. The same core with only 3 GlcNAc attached was detected at *m/z* 2174, which is clearly not as abundant as *m/z* 2419. This core structure was variably extended by a combination of Fuc, Hex, and HexNAc increments, representing residual Le$^{x/a}$ or type 1 units resistant to digestion. Specifically, an increment of $Fuc_2Hex_2HexNAc_1$, which would extend one of the antennae to $Fuc_2(Hex\text{-}HexNAc)_2^-$, afforded the next major peak at *m/z* 3422, whereas a further increment of $Fuc_2Hex_2HexNAc_1$ on the latter gave rise to the signal at *m/z* 4425.

MALDI MS/MS of the core structure at *m/z* 2419 (Fig. 9*A*) revealed a sequential loss of nonreducing terminal GlcNAc from the parent ion and the corresponding b ion without the reducing end PA-tagged fucosylated GlcNAc (*m/z* 1874) to yield eventually a sodiated trimannosyl core ion, $Hex_3HexNAc^+$, at *m/z* 838 with 4 exposed free OH groups, consistent with either a tetraantennary or bisected triantennary core structure (see schematic drawing in Fig. 9*A*). MS/MS of *m/z* 3421 demonstrated that the additional Hex-HexNAc-Hex- unit was extended from only one antenna, as shown by its facile loss, to give a prominent y ion at *m/z* 2160 (Fig. 9*B*). This antenna was difucosylated, and the MS/MS data indicated that two alternative sequences, Fuc-Hex-(Fuc)HexNAc-Hex-HexNAc and Hex-(Fuc)HexNAc-Hex-(Fuc)HexNAc, coexist. The nonfucosylated Gal-GlcNAc unit in the former would most likely be type 1 to make it resistant to endo-β-galactosidase digestion, whereas the internal Hex-(Fuc)HexNAc unit in the latter could be either Le^a or Le^x. Although the *m/z* 838 ion was not apparent, ions common to those afforded by the trimannosyl core structures (Fig. 9*A*) including *m/z* 2160, 1901, 1615, 1356, 1097, and 907 nevertheless firmly established a similar tetraantennary or bisected triantennary structure.

To distinguish further between the two possibilities, the [^{3}H]glucosamine-labeled endo-β-galactosidase-resistant core structures were analyzed by lectin affinity HPLC (Fig. 10),

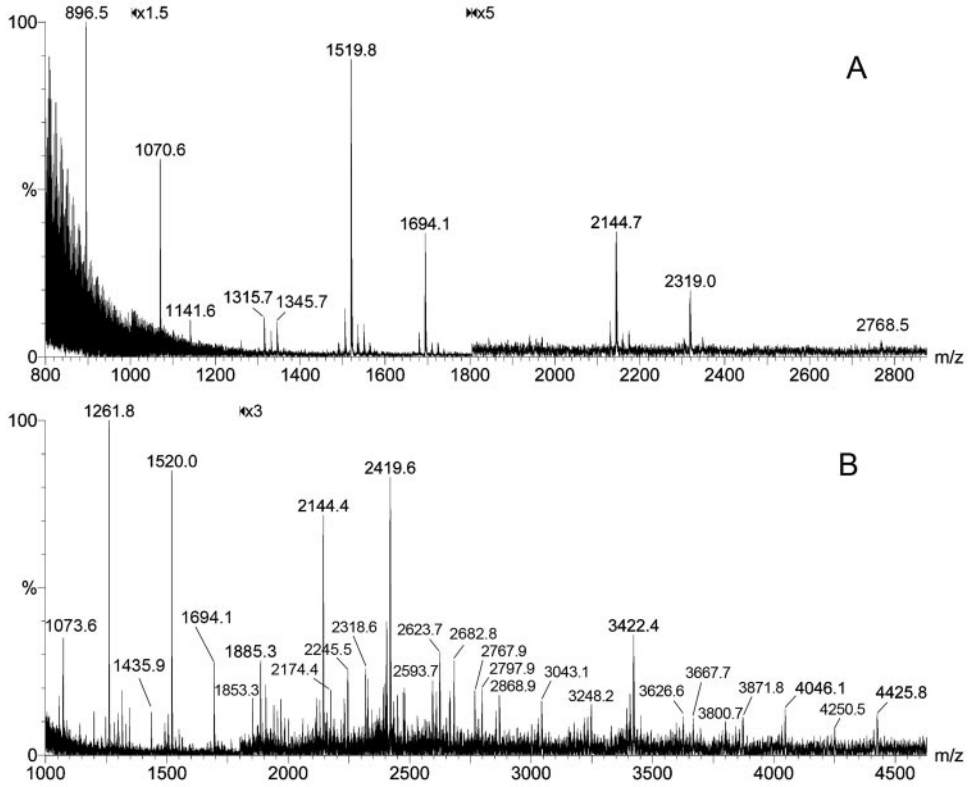

FIG. 7. **MALDI-MS analyses of the permethylated, endo-β-galactosidase-digested products of MLO-N.** The digest was separated into washed-through and retained fractions on a C18 Sep-Pak cartridge. *A*, the aqueous wash fraction contained the released nonreducing terminal fragments, terminating with a nonsubstituted β-Gal at the free reducing end. The signals at *m/z* 896, 1519, 2144, and 2768 correspond to $[M+Na]^+$ of [Hex-(Fuc)HexNAc]$_{1-4}$Hex, respectively, whereas those at *m/z* 1070, 1694, and 2319 reflected an additional Fuc, at 174 units higher. *B*, the 50% aqueous acetonitrile-eluted fraction contained resistant core structures that could be assigned as variably trimmed, PA-tagged tetraantennary trimannosyl core structures. Two of the more prominent signals further subjected to MS/MS analyses (Fig. 9) were *m/z* 2419 and 3422, both of which could be similarly extended with a Hex (*m/z* 2623, 3626), a HexNAc (*m/z* 2664, 3667), a Fuc_1Hex_1 (*m/z* 2797, 3800), a $Hex_1HexNAc_1$ (*m/z* 2868, 3871), a $Fuc_1Hex_1HexNAc_1$ (*m/z* 3043, 4046), a $Fuc_1Hex_2HexNAc_1$ (*m/z* 3248, 4250), and a $Fuc_2Hex_2HexNAc_1$ (*m/z* 3422, 4425). These highly heterogeneous core structures afforded several prompt fragment ions similar to those detected for intact MLO-N (Fig. 4). Molecular ion signals corresponding to released oligosaccharides similar to those detected in the wash fraction (*A*) were also found for this fraction.

taking advantage of the oligosaccharide binding specificity of plant lectins. PHA-E4 binds to biantennary and triantennary *N*-glycans with the third branch on C-3 of β-Man and particularly strongly to those with bisecting GlcNAc (27). In contrast, PHA-L4 binds to triantennary *N*-glycans with the third branch on C-6 of β-Man, and tetraantennary *N*-glycans (27). The PA-tagged core portion obtained on endo-β-galactosidase digestion of [^{3}H]glucosamine-labeled-PA-MLO-N was applied to PHA-E4 and PHA-L4 columns, the results being shown in Fig. 10 together with the elution positions of some reference PA-*N*-glycan chains. On a PHA-E4 column, neither radioactivity nor a PA signal was detected at the elution position of the standard triantennary bisected core *N*-glycan (Fig. 10*A*), suggesting the absence of biantennary glycan chains in the core portion of MLO-N. In contrast, on a PHA-L4 column, a significant portion of the PA signals as well as radioactivity was found at a slightly retarded position on the column (Fig. 10*B*), suggesting the presence of tetraantennary *N*-glycans in the core portion of MLO-N. Similar lectin HPLC analysis with an AAL column (Fig. 10*C*) revealed that the PA-tagged core portions obtained on endo-β-galactosidase digestion were almost completely bound to the column and eluted at the position of α-Fuc1–6-linked *N*-glycans, consistent with the MS data that indicated that almost all of the *N*-glycans are core-fucosylated. Using the same AAL column, it was further demonstrated that essentially all of the radioactivity in the C18 Sep-Pak cartridge H_2O wash fraction containing the endo-β-galactosidase-released terminal fragments of MLO-N was retained (Fig. 10*D*) and eluted as multiple peaks with a buffer containing 5 mM Fuc. The results therefore further confirmed the highly fucosylated nature of MLO-N carbohydrate chains.

MS Analysis of Monosialylated MLO-A1

On anion exchange chromatography, the majority of the acidic MLO was eluted at a position corresponding to monosialylated oligosaccharide, designated as MLO-A1 (Fig. 2). Sugar analysis and quantification indicated that the total glycan content of MLO-A1 was about the same as that of MLO-N, but the additional presence of approximately 1 mol of sialic acid/10 mol of neutral sugars considerably increased the structural heterogeneity. Direct MS analysis of the permethylated intact MLO-A1 was not successful in giving intact molecular ions, but induced cone fragmentation by nano-ESI-MS yielded fragment ions similar to those observed for MLO-N (Fig. 4*A*). Notably, two additional ions were observed at *m/z* 999 and 1622, corresponding to NeuAc-Hex-(Fuc)HexNAc$^+$ and NeuAc-Hex(Fuc)-HexNAc-Hex-(Fuc)HexNAc$^+$, respectively (data not shown). MALDI-MS/MS of the more abundant prompt fragment ions at *m/z* 1261, 1435, 1710, and 1884 gave spectra identical to those acquired for MLO-N, with an abundance of *m/z* 402. The data are therefore consistent with the nonreducing terminal structures of MLO-A1 being very similar to those of MLO-N, with the exception that a portion of the antennae was capped with sialic acid. Because sialyl-Le^a is known to be expressed by SW1116 cells but sialic acid did not contribute to MBP binding, it is reasoned that the presence of a single sialic acid on

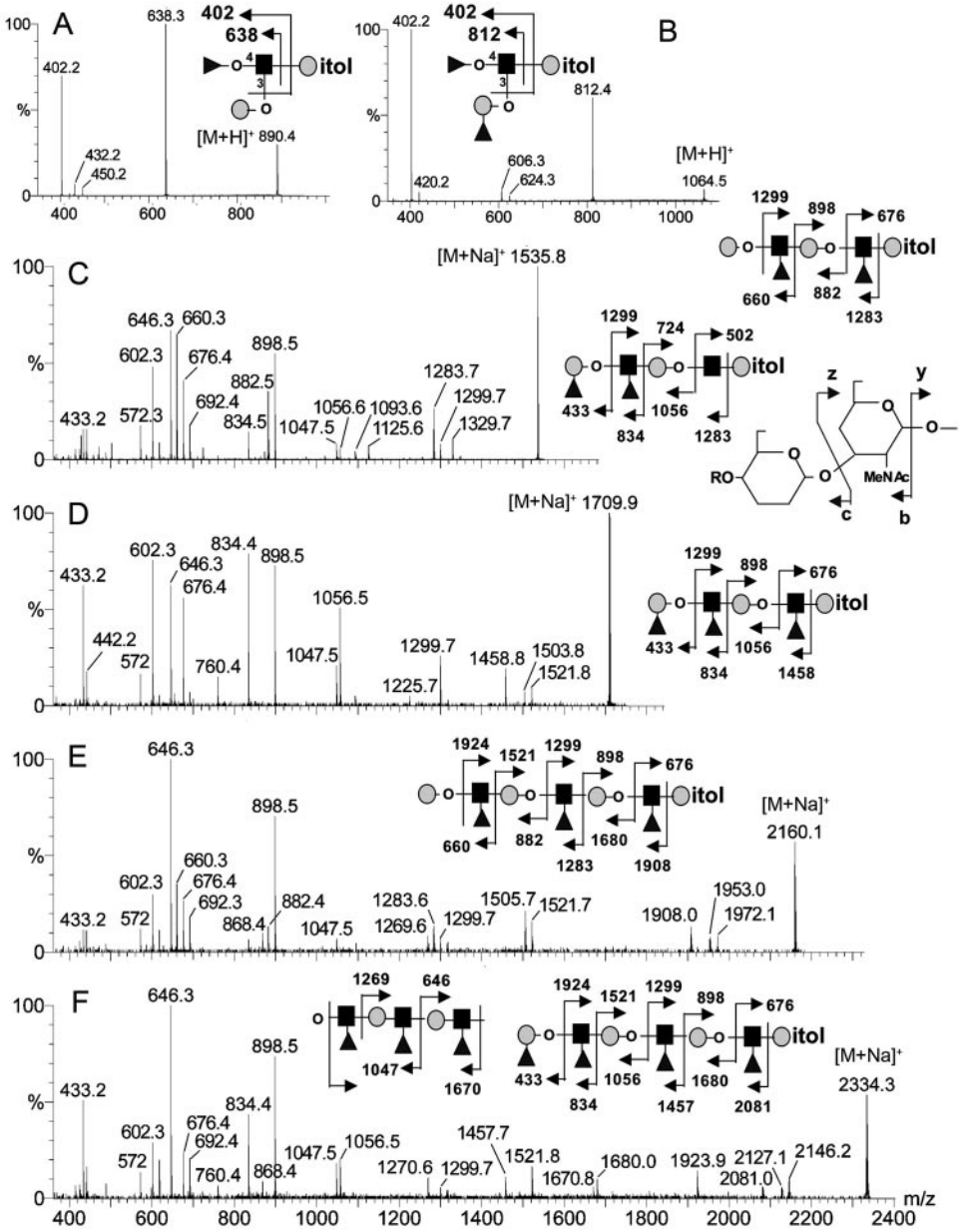

FIG. 8. **MS/MS analyses of the endo-β-galactosidase released nonreducing terminal fragments from MLO-N.** The C18 Sep-Pak wash fraction containing the released fragments was reduced and then permethylated. Protonated oligoglycosyl alditols were detected by nano-ESI-MS and selected for CID MS/MS (only the MS/MS spectra for Le^a-galactitol (*A*) and Le^b-galactitol (*B*) are shown). In separate analyses, sodiated parents were detected by MALDI-MS and selected for CID MS/MS, four representative spectra (*C–F*) being shown. Assignments of major fragment ions observed are illustrated by schematic drawings using *symbols* similar to those adopted for Fig. 5. Glycosidic oxygen was shown to distinguish z and c ion pairs from the more common cleavage producing the b and y ion pairs. Two major isomers of $Fuc_2(Hex\text{-}HexNAc)_2$-Gal-itol are shown in *C*, together with a schematic drawing illustrating the origin of the linkage-specific c and z ions. z and y ions corresponding, respectively, to elimination (minus 206 units) and loss of Fuc (minus 188 units) from parent ions and other primary fragment ions (*e.g.* *m/z* 898) could be additionally detected. The secondary cleavage ion at *m/z* 602 is associated with *m/z* 676.

MLO-A1 did not interfere with its binding to MBP, which was largely contributed to instead by the nonsialylated, highly fucosylated antennae identical to those carried by MLO-N.

To obtain supporting evidence for similar multiantennary core structures, MLO-A1 was treated similarly by endo-β-galactosidase digestion, but after desialylation and aqueous HF defucosylation to allow maximum digestion. Under the conditions employed, core α6-Fuc is known to be relatively resistant to HF treatment compared with α2,3/4-Fuc on the peripheral and terminal sequences, which are readily removed. MALDI-MS analysis of the permethylated digestion products afforded molecular ion signals for both the released fragments as well as the resistant core (Fig. 11). For the nonfucosylated type 2 chain, endo-β-galactosidase should in principle yield only Gal-GlcNAc-Gal (*m/z* 722) and GlcNAc-Gal (*m/z* 518) from the nonreducing termini and internal sequence, respectively. Any Hex-HexNAc extension from these two basic units implies the presence of a type 1 Gal-GlcNAc unit that is resistant to endo-β-galactosidase. Thus, the additional presence of molecular ion signals at *m/z* 1171 and 1621 corresponding to Gal-$(GlcNAc\text{-}Gal)_{2,3}$, and *m/z* 967 and 1417 corresponding to GlcNAc-Gal-$(GlcNAc\text{-}Gal)_{1,2}$ implied an extended type 1 chain, although the possibility of incomplete digestion precluded a firm conclusion. It was also noted that similar digestion of non-HF-treated MLO-N did not give any significant amount of released fragments derived from the internal sequence (Fig. 4), *i.e.* all major fragments detected had either a Gal or fucosylated Gal at the nonreducing end. The data thus suggested that there

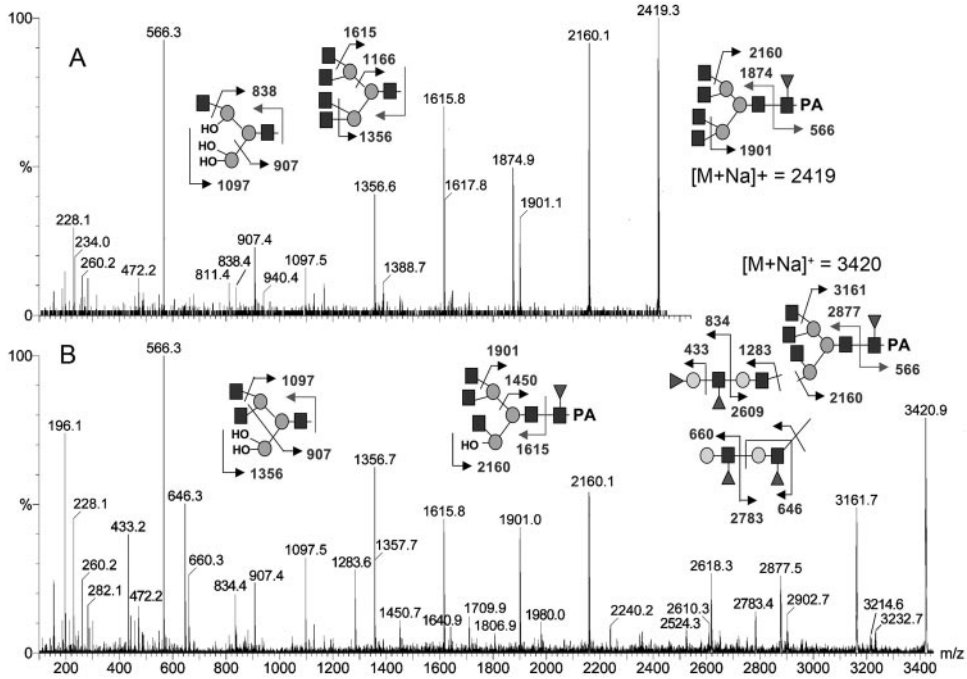

FIG. 9. **MALDI-MS/MS of the two major core structures resistant to endo-β-galactosidase digestion.** Assignments of major fragment ions afforded by the sodiated parent ions are schematically illustrated. *A*, fucosylated trimannosyl core with four exposed nonreducing terminal GlcNAc. Sequential loss of the terminal GlcNAc occurred for the parent and primary b ion at *m/z* 1874. *B*, the same core structure as in *A* but extended at a single antenna with a difucosylated (Hex-HexNAc)$_2$. Direct loss and elimination of Fuc from the parent ion yielded the ions at *m/z* 3232 and 3214, respectively. Sequential loss of the terminal GlcNAc (minus 259 units) and/or the terminal Gal-(Fuc)GlcNAc unit from the parent ion, as well as other more prominent primary ions, also occurred readily. The location of the single extended antennae is not specified in the schematic drawing.

was no significant amount of punctuated gaps in nonfucosylated LacNAc units to allow efficient endo-β-galactosidase digestion without first removing the Fuc. Alternatively, fragments such as (GlcNAc-Gal)$_2$ (*m/z* 967) may be derived through nonspecific HF degradation of the nonreducing terminal Gal of a Gal-(GlcNAc-Gal)$_2$ fragment (*m/z* 1171).

In the higher mass range, a cluster of signals was detected of which the more prominent ones at *m/z* 2245 and 2419 could be assigned as $[M+Na]^+$ of the resistant trimannosyl core with 4 GlcNAc attached, with and without core fucosylation (Fig. 11, *inset*). The basic core structures of MLO-A1 are therefore similar to those of MLO-N, which were identified as the tetraantennary, fucosylated trimannosyl core. A single Hex extension constituted the other major component (*m/z* 2449 and 2623), corresponding to having a Hex-HexNAc unit on one of the antennae. Unlike the case of MLO-N, further extension with Lewis units was not apparent because more complete endo-β-galactosidase digestion of defucosylated, desialylated MLO-A1 would have trimmed off the terminal unit attached to the core via a susceptible LacNAc.

The overall picture is therefore supportive of multiantennary *N*-glycans being the MBP ligands in both the neutral and acidic fractions (Fig. 12). The antennae were extended with highly fucosylated polylactosamine structures, a significant proportion of which terminate at the nonreducing end as the Le$^{a/b}$ epitope and are attached to the core via a nonfucosylated, endo-β-galacosidase-susceptible type 2 LacNAc unit.

DISCUSSION

MBP has been shown to bind only a limited number of endogenous glycoproteins, even though the ligand sugars, *i.e.* Man, GlcNAc, and Fuc, are rather common constituents of various types of glycoproteins and glycolipids. In addition, there has been no report describing the isolation of endogenous oligosaccharides on an MBP affinity column. In this respect, MBP is markedly different from plant lectins, many of which are routinely used as tools for the separation and isolation of oligosaccharides released from various glycoproteins from different sources. During the course of the study on the recognition mechanism of SW1116 cells by MBP, we succeeded in isolating an endogenous oligosaccharide ligand from SW1116 cells with an MBP affinity column, providing us a unique opportunity to study the structure of the endogenous ligand. The elucidated structure was novel and unique, and it represents a new family of tumor-associated carbohydrate antigens.

The initial inhibition studies involving plant lectins and anti-Lewis mAbs of the MBP binding to SW1116 cells suggested strongly that the ligands on the cell surface contain Le^b and Le^a epitopes. To understand the chemical nature of the MBP ligands on the surface of the cells, living cells were surface labeled with biotin, and the biotin-labeled compounds were isolated with an avidin column. Among the surface proteins isolated, a couple of proteins were shown to bind to an MBP column. Interestingly, a predominant portion of these ligands disappeared on treatment with *N*-glycanase, indicating that most of the ligands are carried by *N*-glycans rather than *O*-glycans.[2] We therefore focused on the *N*-glycans, and our current studies showed that the MBP ligands, MLO-N, are large neutral oligosaccharides and highly heterogeneous in molecular size distribution.

N-Glycans of comparable sizes had been described for lactosaminoglycan of band 3 protein isolated from human erythrocytes (30). However, neither band 3 protein isolated from human erythrocytes nor lactosaminoglycan isolated therefrom binds to MBP at all (data not shown). This should be explained by the fact that MBP requires either Man or GlcNAc or Fuc at

[2] R. Inoue, K.-H. Khoo, M. Terada, Nana Kawasaki, B. Y. Ma, S. Oka, T. Kawasaki, and Nobuko Kawasaki, manuscript in preparation.

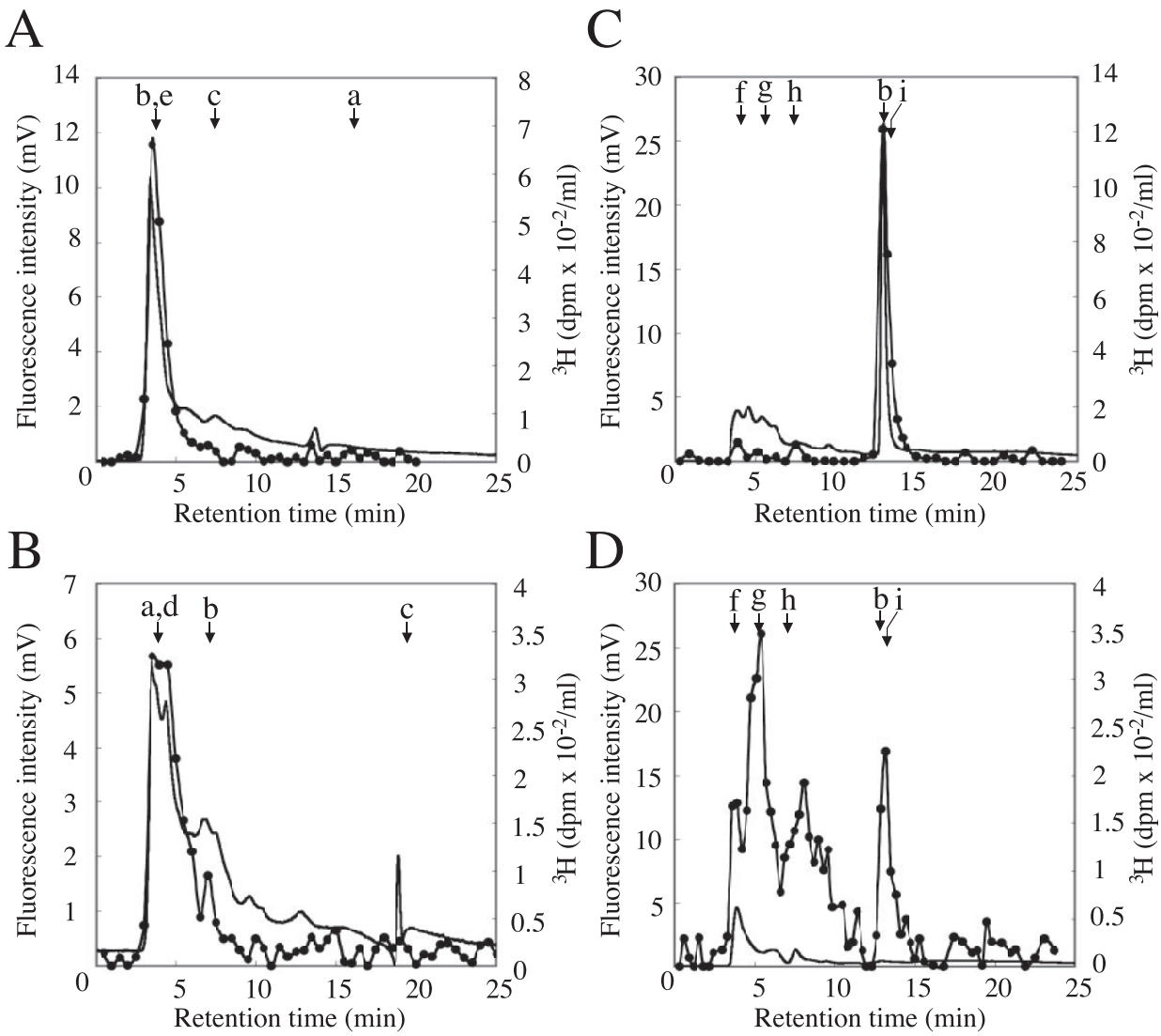

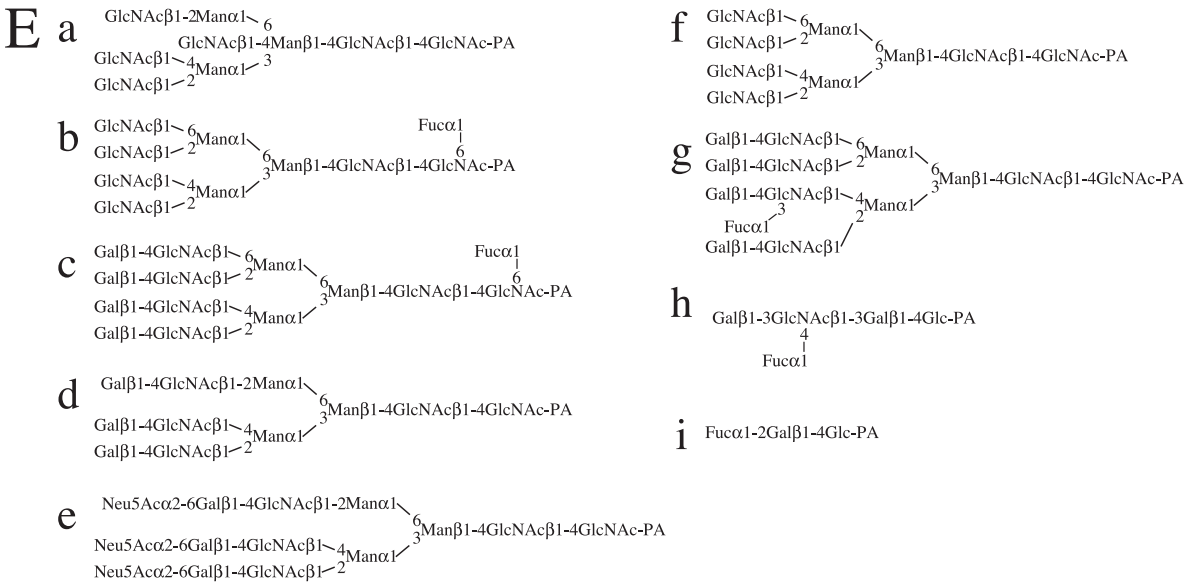

FIG. 10. **Elution profiles of the endo-β-galactosidase digests of [^{3}H]glucosamine-labeled MLO-N on lectin affinity HPLC columns.** The resistant core structures eluted from C18 Sep-Pak in the 50% acetonitrile fraction were fractionated on *A*, an LA-PHA-E4 column (4.6 mm × 15 cm), equilibrated with eluent A (50 mM Tris-H_2SO_4 buffer, pH 8.0), and developed with a linear gradient of 0–100% of eluent B (50 mM

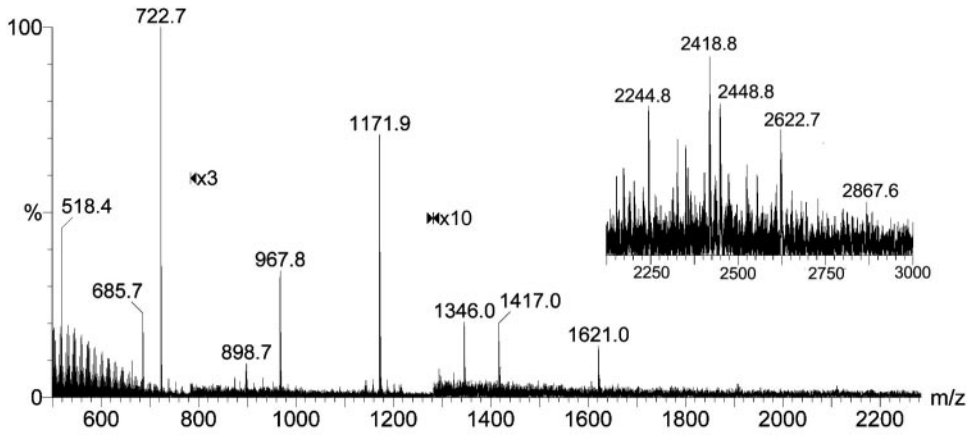

FIG. 11. **MALDI-MS analyses of the permethylated, endo-β-galactosidase-digested products of desialylated and defucosylated MLO-A1.** MLO-A1 was defucosylated with HF and then desialylated with neuraminidase before being subjected to endo-β-galactosidase digestion. The digest was fractionated on a C18 Sep-Pak cartridge similar to for the preparation of MLO-N but eluted with 5% acetonitrile after an aqueous wash. The released fragments were detected in both the wash and 5% acetonitrile fractions, whereas the core structures were only detected in the latter fraction, as shown by the magnified view in the *inset*.

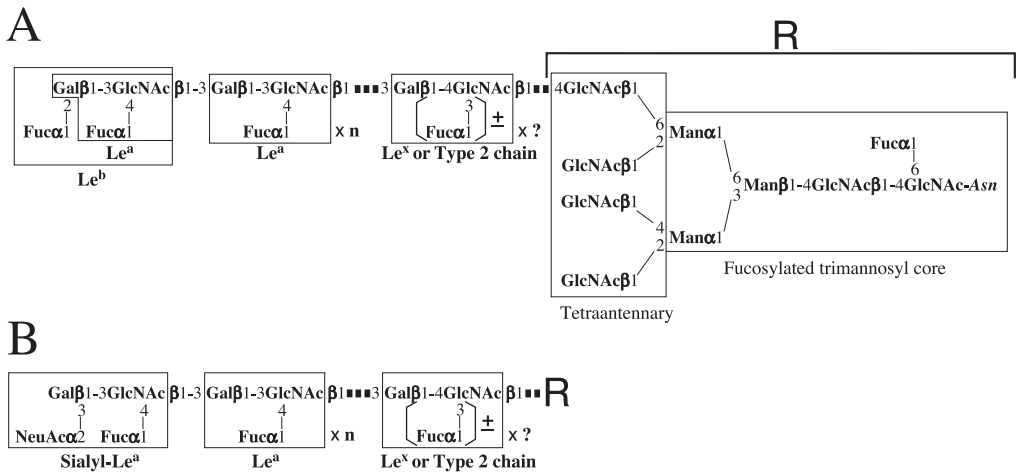

FIG. 12. **Summary of the MLO structure.** *A*, MLO-N. *B*, MLO-A1. *R* denotes the reducing terminal core structure. The MBP ligands on SW1116 cells are mostly composed of tetraantennary core fucosylated *N*-glycans with highly fucosylated polylactosamine type structures. The nonreducing terminal unit is mostly $Le^{b/a}$, a substantial portion of which is carried on extended type 1 chains as multimeric Le^a units (*n*, the maximum number of the repeating Le^a units detected is 4). The inner units are likely to be dominated by type 2 chains and not fully fucosylated (*?*, the number of the Le^x units is not identified, see "Discussion"). The overall carbohydrate structures of the neutral and acidic MBP ligands are very similar except in the nonreducing termini. The acidic ligands are capped with sialic acid to form the sialyl-Le^a structure. Almost equivalent amounts of neutral and acidic fractions could be isolated.

the nonreducing termini of the oligosaccharides chains, but none of these sugars was the major constituent of band 3 carbohydrates, which are composed of a repeating *N*-acetyllactosaminyl structure of $(Gal\beta1–4GlcNAc\beta1–3)_n$. In contrast, SW1116 MBP ligands have very high fucose content, and a predominant portion of the poly-LacNAc type units seems to have a fucose branch. The crucial role of Fuc in the MBP binding was shown clearly by the complete loss of MBP binding activity of MLO-N on chemical defucosylation. However, the presence of the fucosylated branch is not sufficient for MBP binding. Thus, upon digestion of MLO-N with *E. freundii* endo-β-galactosidase, which cleaves only type 2 chain (Galβ1–4GlcNAc) linkages without a Fuc on the GlcNAc, MLO-N lost a large amount of their MBP binding activity, even though they still retained Fuc residues (see Fig. 6*C*). This loss of binding activity on endo-β-galactosidase digestion can be ascribed to the partial cleavage of the backbone polyLacNAc structure (compare Fig. 3*A* and Fig. 6*D*). Defucosylation of MLO-N by HF prior to the endo-β-galactosidase digestion increased the radioactivity in the H_2O eluate from 32 to 57%, suggesting that approximately one-half of the Galβ1–4GlcNAc linkage was masked by a Fuc on the GlcNAc residue.

Tris-H_2SO_4 buffer, pH 8.0, and 0.1 M potassium tetraborate) over 25 min and 100% B from 25 to 40 min at a flow rate of 0.5 ml/min; *B*, an LA-PHA-L4 column (4.6 mm × 15 cm), equilibrated with eluent A (50 mM Tris-H_2SO_4 buffer, pH 8.0) and developed with 100% eluent A for 5 min, and then with a linear gradient of 0–100% of eluent B from 5 to 20 min, and 100% eluent B from 20 to 30 min at a flow rate of 0.5 ml/min; and *C*, an LA-AAL column (4.6 mm × 15 cm). *D*, the wash fraction containing the released oligosaccharides was also fractionated on the same LA-AAL column, as in *C*, both being performed as described in the legend to Fig. 6*C*. In *B* and *C*, the fractions were collected at 0.25 ml/tube, and an aliquot of each fraction was used for determination of ^3H radioactivity. In *A*, *B*, *C*, and *D*, *solid lines* show the PA fluorescence detected at an excitation wavelength of 320 nm and an emission wavelength of 400 nm; *closed circles* show the ^3H radioactivity, and the *arrows* indicate the elution positions of reference PA-oligosaccharides, 10 pmol of each being injected into the columns. *E*, structures of reference PA-oligosaccharides. *a*, asialo, agalacto, bisected triantennary nanosaccharide; *b*, agalactotetraantennary core fucosylated decasaccharide; *c*, asialotetraantennary core fucosylated tetradecasaccharide; *d*, asialotriantennary undecasaccharide; *e*, trisialylated triantennary tetradecasaccharide; *f*, asialo, agalactotetraantennary nanosaccharide; *g*, asialotetraantennary 3′-*N*-fucosyl-GlcNAc tetradecasaccharide; *h*, lacto-*N*-fucosyl pentasaccharide.

Detailed structural analysis of intact MLO proved to be difficult, and our strategy relied instead on detecting the nonreducing terminal sequences and the trimannosyl core structures separately. MS analyses of the latter were relatively straightforward and, in combination with lectin chromatography, have shown that both neutral and acidic MLO are based on mostly tetraantennary complex type structures. Bi- and triantennary structures either do not carry terminal MBP-binding epitopes or do not exhibit sufficient binding affinity or valence for them to be retained on an MBP column. Analysis of the nonreducing terminal epitopes was based on detecting both the fragment ions afforded on direct MS analysis of intact MLO and the oligosaccharide fragments released by endo-β-galactosidase. In both cases, facile sequencing was possible by low energy CID MS/MS of permethyl derivatives with Q/TOF type MS instruments. Sodiated parents gave abundant b and y ions resulting from glycosidic cleavage at HexNAc and, notably, additional c and z ion pairs resulting from cleavage at Gal 3-linked to GlcNAc in type 1 units, if present. A limitation of the current MS/MS sequencing strategy, as applied to isomeric parents, is the lack of specific cleavage at 4 linkages as in type 2 units. Thus, although the presence of the internal type 1 unit, or Le^a, could be determined by detecting the corresponding c and z ions, the coexistence of the type 2 unit, or Le^x, in the isomeric mixtures, could not be ruled out. The presence of the Le^x epitope tends to be indicated by the facile elimination of the Fuc 3-linked to GlcNAc (minus 206 units), but such elimination could occur for any of the multiple Le^x units along the chain.

Taking this limitation into consideration, it is clear that internal type 1 or Le^a units were present in the antennary chains of MLO, but our data could not establish unambiguously whether these were contiguous sequences or sequences punctuated by type 2 units. Irrespective of the internal stretch, a majority was clearly attached to the core via nonfucosylated type 2 units and therefore susceptible to endo-β-galactosidase digestion. Consistent with this conclusion, the fragments released by endo-β-galactosidase or those remaining attached to the core were found to be mostly fucosylated at every HexNAc (Fig. 7). In contrast, the fragment ions directly afforded by intact MLO (Fig. 4) reflected more underfucosylated LacNAc units, particularly but not exclusively at the reducing end. More importantly, our data clearly revealed the nonreducing terminal Lewis unit to be predominantly Le^b and Le^a, as indicated by the high abundance of *m/z* 402 relative to *m/z* 432 and 606 afforded on MS/MS analyses of the ±Fuc-Gal-(Fuc)GlcNAc$^+$ oxonium ion from the intact MLO-N and the protonated ±Fuc-Gal-(Fuc)GlcNAc-galactitol parent ions (Fig. 8, *A* and *B*). MS/MS analyses of the sodiated parents also firmly established that a substantial portion of the MLO antennae were capped by terminal Le$^{b/a}$-Le^a and that these single and extended type 1 terminal units were directly linked to the core via nonfucosylated type 2 units or with an additional internal type 1/type 2 sequence of variable length. Taken together, the major conclusions with respect to the fine structural details of the MBP ligands on SW1116 cells may be summarized as in Fig. 12.

Because MBP recognizes and binds to some colorectal carcinoma cell lines such as SW1116, LS180, and Wider (9), and Colo 205, Colo 201, and DLD-1 (17), but does not bind to normal mammalian cells such as circulating blood cells, it may be reasonable to assume that the MBP ligands characterized in this study represent a tumor-specific carbohydrate antigen. In fact, aberrant glycosylation has been found in essentially all tumor cells so far examined. These antigens include the T (Galβ1–3GalNAcα1-*O*-Ser/Thr), Tn (GalNAcα1-*O*-Ser/Thr), and sialyl-Tn (NeuAcα2–6GalNAcα1-*O*-Ser/Thr) epitopes, the sialyl-Le^a (NeuAcα2–3Galβ1–3[Fucα1–4]GlcNAcβ1–3Galβ1-R) and sialyl-Le^x (NeuAcα2–3Galβ1–4[Fucα1–3]GlcNAcβ1–3Galβ1-R) epitopes, and extended type 2 chains such as Le^x-Le^x (dimeric Le^x; Galβ1–4[Fucα1–3]GlcNAcβ1–3Galβ1–4[Fucα1–3]GlcNAcβ1–3Galβ1–4Glcβ1–1Cer) and Le^y-Le^x (trifucosyl Le^y; Fucα1–2Galβ1–4[Fucα1–3]GlcNAcβ1–3Galβ1–4[Fucα1–3] GlcNAcβ1–3Galβ1–4Glcβ1–1 Cer) (31). In contrast to type 2 chains, which are present as either branched or unbranched poly-LacNAc, type 1 chains (Le^a) have been suggested to exist only at the periphery of type 2 chains (32). However, in later studies, repetitive type 1 chain carbohydrates such as Le^a-Le^a (33) and Le^b-Le^a (34) were found in the glycolipid fraction of Colo 205 cells.

The structures of MLO are very unique and distinct from those of previously reported tumor-specific carbohydrate antigens. First, MLO are present as *N*-glycans but not as glycolipids or *O*-glycans. Second, the tandem repeat region of MLO is much longer than the dimeric or trimeric structure. Third, the tandem repeat consists of the Le^a structure rather than the Le^x structure, particularly at or near the nonreducing termini. Because of these characteristics, the MLO should be considered as representative of a new family of tumor-associated carbohydrate antigens. Another interesting point is the possible relationship with the observation that tetraantennary *N*-linked structures resulting from the addition of side chain GlcNAcβ1–6Manα1–6Man are correlated with the degree of malignancy in essentially all types of cancer (35, 36). The MLO are most likely extended at this particular side chain, and the interaction of MBP with a ligand may be the mechanism associated with the recognition of the tumor cells by a host defense factor, MBP.

Finally, it is interesting to note the differences in the modes of recognition of oligosaccharides by anti-Le^a mAb and MBP. Anti-Le^a mAb recognizes Le^a trisaccharide, 3Galβ1–3[Fucα1–4]GlcNAcβ1, whereas MBP requires the tandem repeat structure of a Le^a trisaccharide for the recognition. These results are consistent with the theory of C. A. Janeway in that the target of recognition in innate immunity (*e.g.* MBP ligands on the SW1116 surface, mannan) represent molecular patterns, called PAMPs for pathogen-associated molecular patterns, rather than particular structures, and receptors that can specifically recognize PAMPs are referred to as pattern recognition receptors (PRRs) (*e.g.* MBP) (4, 37).

REFERENCES

1. Ikeda, K., Sannoh, T., Kawasaki, N., Kawasaki, T., and Yamashina, I. (1987) *J. Biol. Chem.* **262,** 7451–7454
2. Super, M., Thiel, S., Lu, J., Levinsky, R. J., and Turner, M. W. (1989) *Lancet* **2,** 1236–1239
3. Kawasaki, T. (1999) *Biochim. Biophys. Acta* **1473,** 186–195
4. Hoffmann, J. A., Kafatos, F. C., Janeway, C. A., and Ezekowitz, R. A. (1999) *Science* **284,** 1313–1318
5. Wallis, R., and Drickamer, K. (1997) *Biochem. J.* **325,** 391–400
6. Yokota, Y., Arai, Y., and Kawasaki, T. (1995) *J. Biochem.* **117,** 414–419
7. Jack, D. L., and Turner, M. W. (2003) *Biochem. Soc. Trans.* **31,** 753–757
8. Kawasaki, N., Kawasaki, T., and Yamashina, I. (1989) *J. Biochem.* **106,** 483–489
9. Ohta, M., and Kawasaki, T. (1994) *Glycoconj. J.* **11,** 304–308
10. Malhotra, R., Lu, J., Holmskov, U., and Sim, R.B. (1994) *Clin. Exp. Immunol.* **97,** (Suppl. 2) 4–9
11. Kuhlman, M., Joiner, K., and Ezekowitz, R. A. (1989) *J. Exp. Med.* **169,** 1733–1745
12. Hartley, C. A., Jackson, D. C., and Anders, E. M. (1992) *J. Virol.* **66,** 4358–4363
13. Hart, M. L., Saifuddin, M., Uemura, K., Bremer, E. G., Hooker, B., Kawasaki, T., and Spear, G. T. (2002) *AIDS Res. Hum. Retroviruses* **18,** 1311–1317
14. Uemura, K., Yokota, Y., Kozutsumi, Y., and Kawasaki, T. (1996) *J. Biol. Chem.* **271,** 4581–4584
15. Hakomori, S. (1996) *Cancer Res.* **56,** 5309–5318
16. Ma, Y., Uemura, K., Oka, S., Kozutsumi, Y., Kawasaki, N., and Kawasaki, T. (1999) *Proc. Natl. Acad. Sci. U. S. A.* **96,** 371–375
17. Muto, S., Sakuma, K., Taniguchi, A., and Matsumoto, K. (1999) *Biol. Pharm. Bull.* **22,** 347–352
18. Kawasaki, N., Kawasaki, T., and Yamashina, I. (1983) *J. Biochem.* **94,** 937–947
19. Fukuda, M., Dell, A., Oates, J. E., and Fukuda, M. N. (1984) *J. Biol. Chem.* **259,** 8260–8273
20. bio.takara.co.jp/catalog/protocol.asp?ID=338 (in Japanese)
21. Suzuki, J., Kondo, A., Kato, I., Hase, S., and Ikenaka, T. (1991) *Agric. Biol.*

Chem. **55,** 283–284
22. Hewitt, L. F. (1973) *Biochem. J.* **31,** 360–366
23. Ito, M., Ikeda, K., Suzuki, Y., Tanaka, K., and Saito, M. (2002) *Anal. Biochem.* **300,** 260–266
24. Dell, A., Reason, A. J., Khoo, K.-H., Panico, M., McDowell, R. A., and Morris, H. R. (1994) *Methods Enzymol.* **230,** 108–132
25. Goldstein, I. J., and Poretz, R. D. (1986) in *The Lectins* (Liener, I. E., Sharon, N., and Goldstein, I. J., eds) pp. 35–247, Academic Press, Inc., New York
26. Cummings, R. D. (1999) in *Essentials of Glycobiology* (Varki, A., Cummings, R., Esko, J., Freeze, H., Hart, G., and Marth, J., eds) pp. 455–467, Cold Spring Harbor Laboratory Press, Cold Spring Harbor, NY
27. Sharon, N., and Lis, H. (2003) in *Lectins* (Sharon, N., and Lis, H., eds) 2nd Ed., pp. 63–103, Kluwer Academic Publishers, Dordrecht, The Netherlands
28. Childs, R. A., Drickamer, K., Kawasaki, T., Thiel, S., Mizuochi, T., and Feizi, T. (1989) *Biochem. J.* **262,** 131–138
29. Dell, A. (1987) *Adv. Carbohydr. Chem. Biochem.* **45,** 19–72
30. Fukuda, M., Dell, A., and Fukuda, M. N. (1984) *J. Biol. Chem.* **259,** 4782–4791
31. Hakomori, S. (2001) in *The Molecular Immunology of Complex Carbohydrates-2* (Albert, M. W., ed) pp. 369–402, Kluwer Academic Publishers, Dordrecht, The Netherlands
32. Kannagi, R., Levery, S. B., and Hakomori, S. (1985) *J. Biol. Chem.* **260,** 6410–6415
33. Stroud, M. R., Levery, S. B., Nudelman, E. D., Salyan, M. E., Towell, J. A., Roberts, C. E., Watanabe, M., and Hakomori, S. (1991) *J. Biol. Chem.* **266,** 8439–8446
34. Stroud, M. R., Levery, S. B., Salyan, M. E., Roberts, C. E., and Hakomori, S. (1992) *Eur. J. Biochem.* **203,** 577–586
35. Fernandes, B., Sagman, U., Auger, M., Demetrio, M., and Dennis, J. W. (1991) *Cancer Res.* **51,** 718–723
36. Granovsky, M., Fata, J., Pawling, J., Muller, W. J., Khokha, R., and Dennis, J. W. (2000) *Nature Med.* **6,** 306–312
37. Lee, R. T., Ichikawa, Y., Kawasaki, T., Drickamer, K., and Lee, Y. C. (1992) *Arch. Biochem. Biophys.* **299,** 129–136